

The Fabrication of a Lab-on-a-Chip Device to Investigate the Invasive Capability of Hyphae in Different Oxygen Levels

Qituo Ding

A thesis submitted in accordance with the requirements of the
University of Canterbury for the degree of

Master of Science in Biochemistry

February 2020



Abstract

Fungi and oomycetes, which can grow invasively, can lead to some of the most devastating die-offs and extinctions of both animals and plants. In their natural environment, such as soil, and during the infection, they may be confronted with low levels of atmospheric oxygen, which may alter their growth behaviour.

The aim of this research was to develop a lab-on-a-chip device, which can control the oxygen levels around fungi or oomycetes. The chip designed in this work has one main channel for the growth of hyphae and flow of the media, feeding into this are two gas channels, which enable manipulation of oxygen concentrations in the main channel.

To demonstrate the applicability of this device, the oomycete *Achlya bisexualis* was inoculated on the chip for a preliminary investigation of the growth behaviour of hyphae at different oxygen levels. Hyphal growth rate and diameter were measured at different flow rates and shown they could not be affected by the flow rates.

The response of the hyphae to the oxygen gradient in the channel was characterised by light microscopy. A change of hyphal behaviour was found due to the oxygen gradient. Some hyphae, which were growing in a high oxygen concentration area, changed their growth directions towards to hypoxic area, suggesting that *A. bisexualis* hyphae were more likely to grow towards hypoxic conditions. Similar to their ability to avoid barriers in their growth path, they might also have the ability to sense the surrounding oxygen concentrations.

The work presented in this thesis provides a device that could lead to a better understanding of fungal and oomycete growth behaviour at different oxygen levels and may open the way to the improvement of existing antifungal therapies or new approaches to tackling their invasive capabilities.

Acknowledgements

There are so many people I would like to thank for their great contributions to my research and life during my Masters. First and foremost, I would like to express my sincere appreciation and gratitude to my supervisor, Ashley Garrill and my associate supervisor, Volker Nock. Without you, I might not have the opportunity to work on this research and miss the chance to get into the world of research life.

To Ashley, thank you so much for supporting me throughout the duration of my undergraduate, postgraduate and Masters. Thanks for being patient to answer all my silly questions and lifted me up with your words of encouragement when I was in deepest doubt. Your kindness and imperturbation will always stand as a model for me. It is a privilege for me to work with you.

To Volker, I am extremely lucky to have you as my supervisor. Thank you for being so nice and providing much-needed engineering advice for the fabrication method to complete this thesis. I really appreciate helping me and providing so many ideas for this project.

I would also like to thank the fantastic people working in the Nanofabrication Laboratory, especially Helen Devereux and Gary Turner, for their technical assistance. Having you in the lab was great.

Next, I wish to make a particular thanks to people in my office. Louise, thank you so much for your wisdom and support on the design of the chip. This work might take much longer if I did not have you. To Yiling, thank you for your tremendous support for the optimization of this research, especially when it came to nothing. This research could not be the same without you. Thanks to Ayelen, Liz, Debolina and Annabella, for their generous help and knowledge. The working environment is enjoyable and productive all because of you.

Finally, my greatest thanks to my parents who have given me so much love and support all my life. Thank you for your unconditional and unwavering support, encouragement, and thank you for never turning back on me.

Abbreviations

Abbreviations used in this thesis are listed here for easy reference.

DI	De-ionized
EPR	Electron paramagnetic resonance
ER	Endoplasmic reticulum
ETFE	Ethylene tetrafluoroethylene
HBO	Hyperbaric oxygen
IPA	Isopropanol alcohol
LOC	Lab-on-chip / Lab-on-a-chip
PC2	Physical containment level 2
PDMS	Polydimethylsiloxane
PE	Polyethylene
PGMEA	Propylene glycol monomethyl ether acetate
PS	Polystyrene
PtOEPK	Platinum (II) octaethylporphyrinketone
PYG	Peptone -yeast- glucose
PVP	Polyvinylpyrrolidone
RTDP	Ruthenium tris(2,2'-dipyridyl) dichloride hexahydrate
TMCS	Trimethylchlorosilane

List of Figures

- 2.1:** Schematic represents of hyphal tip growth. The most crucial feature of hyphal tip growth is the movement of material towards the apex to create new cell wall, new membranes and new cytoplasmic components. Cell expansion is driven by turgor pressure and yielding of the wall at the apex to that pressure (Hibbett, 2012). **8**
- 3.1:** A schematic of the channel geometry of the chips used by Orcheston-Findlay et al. (2018) to study the effect of oxygen gradients on cancer cell cultures. **24**
- 3.2:** A schematic of the newly designed chip. The chip has three channels; each channel has the same height, 100 μm , and same width, 1000 μm . A central channel is used to grow the hyphae while the gas channels are used to control the oxygen concentration in the central growth channel. **24**
- 3.3:** A completed silicon mould master. **26**
- 3.4:** Photographs of the setups used for casting PDMS. a) the stack including the metal stage, the PE sheet, the ring, and the wafer; b) PDMS was poured on the wafer within the ring and enclosed with a weight at the top; c) Leaking of PDMS between the ring and the wafer. **28**
- 3.5:** A photo of the completed chip that was designed and fabricated for this thesis. To improve visibility the main channel and seeding area were filled with red dye. One gas channel was filled with green dye, while the other gas channel was filled with blue dye. **29**
- 3.6:** The various components that made up the fluidic system and their position in the system. Fluidic connections are solid black, gas are blue, and electrical connections to the computer are shown in yellow. **31**
- 4.1:** Oxygen gradient on the chip. a) The raw signal from the RTDP fluorescent measurement at $t = 0$; b) The raw signal from the RTDP fluorescent measurement at $t = 60$ mins; c) oxygen gradient formed in the channel (black line), and the predicted oxygen gradient in the channel according to the Stern-Volmer equation (yellow dotted). **36**
- 4.2:** Hyphae growth rate at different media flow rates. There was no significant effect on growth rate at the different flow rates. **38**

4.3: The effect of different media flow rates on hyphal diameter. The diameter was measured 100 μm behind the hyphae tips. Flow rate had no significant effect on diameter. **39**

4.4: Hyphae growing straight in the channel at a flow rate of 30 $\mu\text{L}/\text{min}$. Time interval of each images was approximately 60 minutes. **41**

4.5: The growth behaviour of hyphae toward the more hypoxic environment. In the Figure the upper part of the channel had high oxygen and the bottom part of the channel had low oxyge. Image (a) to (e) were taken at time 0, 30, 60, 90, 120 minutes, respectively. **44**

4.6: The growth behaviour of hyphae in the normoxic environment. Image (a) to (d) were taken at time 0, 30, 60, 90 minutes, respectively. **45**

4.7: The effects of the formation of air bubbles on hyphal growth behaviour. Images were taken at a) the back; b) the front of the hyphal growth in the same experiment and the same time. **47**

4.8: Hyphae stopped growing at the entrance of the main channel due to the RTDP in the media flow. a) microscopic and fluorescent images were taken at $t = 0$; b) microscopic and fluorescent images were taken at $t = 60$ minutes; c) microscopic and fluorescent images were taken at $t = 120$ minutes. **49**

Table of Contents

Chapter 1 Introduction	1
1.1 Overview	1
1.2 Thesis contribution	2
1.3 Thesis structure	2
Chapter 2 Background	4
2.1 Background to fungi and oomycetes	4
2.1.1 Fungi and oomycetes	4
2.1.2 Fungal life cycle	6
2.1.3 Tip growth	7
2.1.4 Invasive and non-invasive tip growth	9
2.1.5 Hypoxia during tip growth of hyphae	9
2.1.6 Study invasive growth of hyphae	12
2.1.7 Fungal infection treatment strategies	13
2.2 Introduction to microfluidic technology	14
2.2.1 Applications of the chip	14
2.2.2 PDMS	15
2.2.3 Photolithography	16
2.2.4 Soft-lithography	16
2.2.5 Etching	17

2.3	Oxygen measurement methods	17
2.3.1	Theory of gas solubility	19
2.3.2	Gas pressure in the channels.....	20
2.4	Aims of this thesis	21
Chapter 3	Methods and Materials	22
3.1	Design of the chip.....	22
3.2	Fabrication of the chip	25
3.4	Microfluidic experimental setup.....	29
3.5	Oxygen gradient on the chip	32
3.6	Maintenance of <i>Achlya bisexualis</i> cultures	32
3.7	Inoculation of <i>A. bisexualis</i> onto the chips.....	33
3.8	Image collection and processing.....	33
3.9	Temperature control	33
Chapter 4	Results and Discussion	35
4.1	Measurement of the Oxygen concentration of the chips.....	35
4.2	Hyphal growth rate against different media flow rate	37
4.3	Hyphal diameter in different media flow rate	39
4.4	Hyphal growth behaviour in hypoxia	42
4.5	Experiment Issues.....	46
Chapter 5	Thesis Conclusion and Future Work.....	50
5.1	Thesis summary and conclusion	50
5.2	Future work.....	52
Reference	53

Chapter 1

Introduction

1.1 Overview

The number of virulent infectious diseases that can be found in natural populations and managed landscapes have been increasing every year over the last few decades. Those diseases which are mostly caused by fungi and oomycetes are a worldwide threat to both animals and plants (Pennisi, 2010). As fungal infections are causing widespread population declines in plants and animals, it is critical to investigate their pathogenesis in order to reduce their economic effects and to conserve global biodiversity. It has been suggested that most of the eukaryotic human fungal pathogens are considered obligate aerobes, which means that oxygen levels during fungal pathogenesis may affect their growth behaviour. This is because in their natural environment, such as in the soil or during the infections, they may be confronted with low levels of atmospheric oxygen. In other words, cellular hypoxia may play a vital role during fungal infections or in their pathogenic growth. Therefore, tip growth, which is the process by which fungi and oomycetes grow, could be affected by cellular oxygen concentration. This suggests that cyclic hypoxia may affect their invasive and pathogenic capability.

Previous work has used sensing pillars to measure the protrusive force in the oomycete *Achlya bisexualis* under standard atmospheric oxygen levels in order to understand the invasive capability of individual hyphae. Due to the potential importance of the levels of oxygen, it is important to consider the impact of changes in oxygen concentration on invasive growth. This research aims to study the invasive capability of hyphae in different oxygen concentrations. This thesis describes the design and the fabrication of a lab-on-

a-chip device, which can control the oxygen concentration around hyphae, and a preliminary investigation of the growth behaviour of hyphae at different oxygen levels.

1.2 Thesis contribution

The primary contribution of this thesis is the development of a lab-on-a-chip device which can control the oxygen levels around fungi or oomycetes. With this control system, the growth behaviour of oomycete *Achlya bisexualis* under different oxygen concentrations can be studied. This extends previous studies (Tayagui, Sun, Collings, Garrill, & Nock, 2017), which have used sensing pillars to measure the protrusive force of fungi and oomycete growing on the chip. However, in those experiments, the hyphae were under atmospheric conditions with an oxygen concentration of approximately 21%. As different oxygen levels may alter the hyphal growth behaviours of fungi and oomycetes, this work provides an important first step for future lab-on-a-chip devices that enable the measurement of growth and protrusive force under different oxygen regimes. A better understanding of fungi and oomycete growth behaviour at different oxygen levels may open the way to the improvement of existing antifungal therapies or the design of new approaches.

1.3 Thesis structure

The contents of each chapter are shown in this section in order to guide the reader through this thesis.

Chapter 2 – Background. This chapter introduces fungi and oomycete, their life cycle, describes how they affect animals and plants by invasive tip growth, and their adaptation in hypoxia is characterized. Following this, a review of the mechanisms of tip growth, the differences between invasive and non-invasive tip growth and strategies to treat fungal infections is presented. This chapter also introduces the theory relating to the microtechnology aspects of this work. The mechanisms of silicon wafer production and development used in this project are described. The oxygen concentration measurement in the liquid is then discussed in terms of gas solubility, pressure and temperature.

Chapter 3 – Methods and Materials. This chapter introduces the chip design and fabrication process, and a microfluidic system set up for the generation of an oxygen gradient on the chip. Maintenance of *Achlya bisexualis* cultures and inoculation of them are also described in this chapter.

Chapter 4 – Results and Discussion. This chapter describes the capability of the microfluidic oxygen-control system. Oxygen gradient data are presented, and the results of hyphal growth behaviour in the microfluidic chip with an oxygen gradient are described.

Chapter 5 – Thesis Conclusions and Future Work. This chapter presents the conclusions resulting from this research and further work.

Chapter 2

Background

2.1 Background to fungi and oomycetes

This section provides a background on the complex biology behind the tip growth of hyphae of fungi and oomycete. The life cycle of fungi and oomycetes, tip growth in atmosphere and hypoxia, how pathogenic fungi adapt to hypoxia, and fungal infection treatment strategies are described. Technologies used to study hyphal invasive growth and their adaptation to hypoxia are introduced. More specific literature reviews related to each technology are included in their relative introductions.

2.1.1 Fungi and oomycetes

Fungi are one of the oldest and largest groups of living eukaryotic microorganisms. This ancestral organism diverged from a common ancestor with the animals about 800 to 900 million years ago. It is unclear how many species of fungi there are on our planet now. However, it has been stated that more than 99,000 species of fungi have been discovered and described. Also, new species are found at a rate of approximately 1,200 annually (Blackwell, 2011). Nowadays, the effect of fungi to human life is becoming more and more significant. This is because fungi can grow invasively, which leads to disease and death of both plants and animals. In the 19th century, late blight caused the Irish potato famine, leading to starvation, economic ruin and downfall of the English government (GrÜNwald, Goss, & Press, 2008).

Moreover, in the twentieth century, Dutch elm blight and chestnut blight caused by those diseases distorted many urban and forest landscapes. Recently, some exotic diseases caused by fungi have caused several of the most severe die-offs, and extinction of flora and fauna ever witnessed. Studies show that fungal infections are emerging as pathogens across diverse taxa. Those include bees (Cameron et al., 2011), soft corals (Kim & Harvell, 2004), and many species of plants (Rizzo & Garbelotto, 2003; Wills, 1993). Thus, it seems that pathogenic fungi are having a pronounced effect on the global biota (Fisher et al., 2012).

Diseases caused by the pathogenic fungi also have severe effects on animal health as they could grow on and in both invertebrate and vertebrate animals. White-nose syndrome in bats was first found in 2007 in New York State (Blehert et al., 2009). The ascomycete fungus *Geomyces destructans* is the cause of this disease, leading to mass mortalities of bats (Lorch et al., 2011). It has also been shown that the number of bats, which are affected by white-nose syndrome have decreased by over 70% and some bat species might face extinction within the next few years (Frick et al., 2010).

However, it should also be noted that fungi may also play an essential role in ecosystem dynamics as many fungi can attack insects and nematodes to keep the populations of those animals under control. Insect-attacking fungi, also known as entomopathogens, are present in several fungal phyla including *Ascomycota*, *Chytridiomycota* and *Zygomycota*. Some of these can change the behaviour of insects. Researchers have found that the pathogenic fungi, *Ophiocordyceps unilateralis*, which is specific to ants, can alter the behaviour of the ant host leading to their death (Evans, Elliot, & Hughes, 2011). This so-called zombie fungus can manipulate their victims and make them die in an exposed position. The hypocrealean fungus *Beauveria bassiana* is another well-known microbial entomopathogen used as an insect pests control agent. Also, because of its effectivity, this species has become a successful commercial product (Jackson et al., 2010).

Oomycetes, also known as water moulds, are a group of fungus-like eukaryotic microorganisms. These can cause diseases that can have a profound effect on agriculture as well as aquaculture. The most notorious species, *Phytophthora infestans*, which triggered the Irish potato famine, has been described above. Other notable species can threat native tree species, for instance, *Phytophthora palmivora* can lead to cocoa black pod and *Phytophthora ramorum* has been found causing the sudden oak death (Rizzo & Garbelotto, 2003). Diseases such as Saprolegniosis and epizootic ulcerative syndrome,

also known as water moulds disease, are the most common diseases of freshwater fish caused by oomycetes. Since aquaculture has become one of the world's fastest-growing food sectors, the order Saprolegniales such as *Saprolegnia*, *Achlya* and *Aphanomyces* are a significant threat to the aquaculture industry as they are particularly pathogenic to animals (Phillips, Anderson, Robertson, Secombes, & van West, 2008).

2.1.2 Fungal life cycle

The pathogenic fungi and oomycete can successfully survive for a long time, mainly because of their capacity to adapt to overcome host resistance. This may suggest that they have high evolutionary potential. Their flexible mating systems may be one reason for their success.

Fungi and oomycetes life cycles are unique and complex as they can reproduce either sexually or asexually. The growth of fungi usually starts with spores. They may be formed via a sexual process through meiosis to generate meiospores or an asexual process through mitosis to produce mitospores. During sexual reproduction, they can be either homothallic or heterothallic. Many fungi produce more than one type of spore during their life cycles. Spores are often produced from inside or upon a mature fungal fruiting body, and they can be released into the surrounding environment, where they could divide and synthesize microscopic tubular filaments called hyphae. Hyphae are root-like threads composed of haploid cells which can grow by elongation either in horizontal or vertical directions. The hyphae may branch as they grow, and the branch forms a new hypha. A mass of hyphae which is not in a reproductive structure is called a mycelium. They can grow through and across substrates or food sources, secreting enzymes that can break down complex materials into simple compounds, which can be used and absorbed back through the fungal cell wall and plasma membrane. In the laboratory, a mycelium that grows in an unimpeded manner can usually form a circular colony on a solid substrate to support the growth of fungi. Researchers often use agar, a gelatinous material derived from seaweed, with required nutrients to grow fungal mycelia in culture.

Most of the hyphae elongate at their tips, growing outwards from the point of establishment. This so-called tip growth could be one of the reasons for the relatively uniform of hyphal diameter. Hence, researchers sometimes use hyphal diameter to

monitor the health conditions of fungi. Some fungi can grow exclusively as yeast cells. These can reproduce asexually by budding or fission. In contrast to the tip growth of hyphae, yeast-like growth shows a wall growth over the entire cell surface, and results in a spherical or ellipsoid cell. In addition, there are some fungi which can switch between sexual or asexual reproduction depend on different environmental conditions (Uchida, Bartnicki-García, & Roberson, 2004 temperature and moisture).

2.1.3 Tip growth

The continuous cell extension maintains the characteristic shape of hyphae at hyphal tips (Uchida et al., 2004). This extension at the apex (also known as tip growth) means that hyphae are polarised structures. It has also been found that the hyphal form (resembling a drill bit) is related to their pathogenicity in plants and animals, so the filamentous form is crucial for the invasion into host cells (Garcia-Vidal, Viasus, & Carratalà, 2013). Super-resolution microscopy has indicated that filamentous fungal cells could maintain their cell polarity at the tips by repeating transient assembly and disassembly at the polarity site (Takeshita, 2016).

During tip growth, each hypha at the leading edge is growing into the environment in order to search for food for survival, while at the back, the hyphae are connecting to form a three-dimensional network which can extract nutrients and other materials from the surrounding medium (Lew, 2011). Tip growth is considered as a complex process involving turgor pressure and localized tip yielding, which leads to the formation of cylindrical cells or hyphae (Lew, 2011). The pressure is an essential thermodynamic state property in all organisms. For those cells that do not have a cell wall, excessive pressure will lead to cell lysis or cell death. However, in cells with a cell wall, an internal hydrostatic pressure (which is also known as turgor pressure) can provide both mechanical support for free-standing structures and a force which can result in cellular expansion, substrate penetration or other processes. The turgor pressure can be created by osmosis due to the response to the concentrations of osmotically active substances (or osmolytes) are being higher within the cell than the outside of the cell. The cell wall at the hyphal tip has viscoelastic properties and yields to the internal turgor pressure within the hypha. Behind the tip, the cell wall is rigid so that it can resist the turgor forces because of the osmotic flow of water into the hypha. A vital aspect of the pathogenicity of oomycetes and fungi

is that hyphae can grow invasively through the host tissue. The invasive growth of fungi requires the enzymatic breakdown of host tissue as well as the protrusive force exerted by the hyphae. The protrusive force is thought to arise due to turgor pressure and increased yielding (through reduced resistance) of the tip to that pressure. Increased yielding in both oomycetes and fungi is thought to come about through modifications to both the cell wall and the cytoskeleton (Walker, Chitcholtan, Yu, Christenhusz, & Garrill, 2006). Researchers have found that the force generated by turgor is sufficient for pathogenic fungi to penetrate and ramify throughout host tissue (Bastmeyer, Deising, & Bechinger, 2002).

Tip growth requires a sequential supply of proteins and lipids to the hyphal tip for synthesis and insertion of the new wall and new membranes. This complex and highly organized process is supported by the actin and microtubule cytoskeleton and polarity marker proteins within the cytoplasm behind the tip as well as other cytoplasmic organelles and their migration towards the hyphal tip (Takeshita, 2016). Figure 2.1 represents an overall molecular model of hyphal growth. Briefly, proteins and lipids move rapidly towards the tip of the hyphae to create new membranes, new cell wall and new cytoplasmic components. Most of those materials are transported in vesicles by the endoplasmic reticulum (ER) and Golgi organelles. These vesicles are then delivered to the apical vesicle cluster (in fungi also called the Spitzenkörper) via microtubules which are driven by motor proteins (Hibbett, 2012).

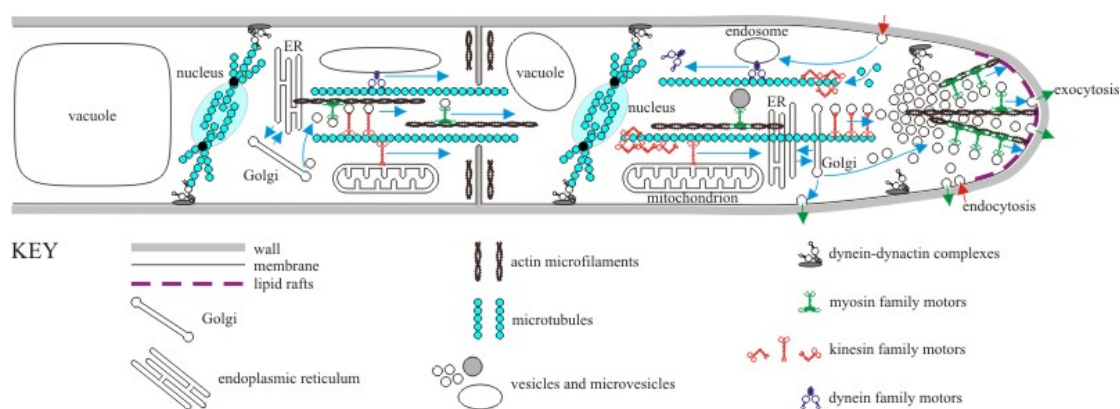


Figure 2.1 Schematic representation of hyphal tip growth. The most crucial feature of hyphal tip growth is the movement of material towards the apex to create new cell wall, new membranes and new cytoplasmic components. Cell expansion is driven by turgor pressure and yielding of the wall at the apex to that pressure (Hibbett, 2012).

2.1.4 Invasive and non-invasive tip growth

As a fungus/oomycete grows into and explores its environment in the search for new nutrients there may be a necessity for tip growth to occur in a range of environments some of which may provide unique difficulties. Invasive growth is a term used to describe the growth of hyphae through solid/semi-solid media. Compared to non-invasive growth, invasive growth requires the ability to generate more force in order to overcome the resistance of the media. In some instances, the force required could be enormous to enable penetration of the surroundings (Heath & Geitmann, 2000). Researchers have found that in the case of appressoria (penetrative hyphae) which can penetrate through Mylar®, the estimated yield stress reached to 50-80 MPa (Goriely & Tabor, 2006). Recently, the protrusive force of *Achlya bisexualis* was measured using Lab-on-a-chip technology. The force was ranging from 0.5 to 10 μ N during invasive tip growth (Tayagui et al., 2017). Those data mean that invasive tip growth can generate a more significant force required to penetrate through solid media, relative to non-invasive tip growth.

The mechanisms of how this greater force is generated are still unclear. However, it is clear that in order to grow through solid media, the protrusive force must not only exceed the withholding capacity of the cell wall but also have sufficient force to penetrate. One theory suggests that the cell wall is playing an important role (Harold, 1997). Instead of the force of pre-existing turgor pressure being absorbed by the cell wall, the force can transfer through a softer cell wall. Therefore, less of the force of turgor will be absorbed by the wall, so that more of the force will be exerted onto the surrounding environment.

2.1.5 Hypoxia during tip growth of hyphae

Oxygen is essential for life, especially for eukaryotic organisms. It plays an essential role in the generation of chemical energy (Raymond & Segrè, 2006) in mitochondria during cell respiration as well as the biosynthesis of compounds such as sterols, NAD, polyunsaturated fatty acids, porphyrin and other materials which needed for the cell. Therefore, the amount of available oxygen in the eukaryotic cells is a crucial factor which could affect overall cellular metabolism.

Oxygen level in a given environment is often described as anaerobic (or anoxic), hypoxic (available oxygen reduces to a deficient level compared to oxygen concentrations of the atmosphere), or normoxic (atmospheric oxygen level, generally 21% O₂). It is generally agreed that hypoxia occurs at the site of infection of fungi and oomycetes so that both host and microbial pathogen cells may have a significant high environmental stress (Nizet & Johnson, 2009). However, an absolute oxygen concentration is difficult to measure *in vivo*, and the oxygen levels are different in various anatomical location and distinct pathologies. Hence, localised hypoxia is very difficult to define. Generally, in healthy human tissue, oxygen levels between 2.5 to 9 per cent are considered as normoxic, while oxygen levels below 1 % are considered as hypoxic (Grahl, Shepardson, Chung, & Cramer, 2012). In a healthy human lung, which could also be described as the original deposition site of many human fungal infections, the levels of oxygen are approximately 14% (Jain & Sznajder, 2005).

In human tissues, hypoxia occurs when oxygen consumption exceeds delivery, and is often caused by an interruption of the blood supply (Chang, Jurisica, Do, & Hedley, 2011). This may lead to cell apoptosis. During fungal infection, hypoxia occurs when an invading microbe interacts with host cells, leading to tissue damage because of inflammation, thrombosis, and necrosis, which could prevent tissue perfusion at the site of infection and decrease available oxygen concentrations (Nizet & Johnson, 2009).

Researchers have found that most eukaryotic human fungal pathogens are generally obligate aerobes, suggesting that oxygen levels during fungal pathogenesis may be an important factor. Also, human fungal infections often occurred under hypoxic conditions, indicating that fungi associated with these infections may be more likely to grow invasively in a low oxygen concentration environment. *Candida albicans*, for example, is one of the most frequently occurring human fungal pathogens and is often found located at the human gastrointestinal tract, which is a region of hypoxia (Karhausen et al., 2004). Also, *Cryptococcus neoformans* can lead to cryptococcal meningitis in the human brain, which is an area that oxygen concentrations are much lower than the atmosphere. These observations indicate that those human pathogenetic fungi may grow invasively with reduced oxygen levels.

Additionally, two related studies of murine invasive pulmonary aspergillosis (IPA) further supports the idea that fungal pathogens may face reduced oxygen levels during pathogenesis. Those studies showed that an *Aspergillus fumigatus* strain which could

previously produce luciferase *in vivo* stopped its production after they infected mouse lungs. This observation may suggest that severe tissue damage caused during infections may lead to the reduction of oxygen availability. Because of the fact that oxygen is vital for the light-producing luciferase reaction, the lack of luminescence may be attributable to hypoxia at the site of infection (Ibrahim-Granet et al., 2010). Another murine chemotherapeutic model of IPA could be a shred of indirect evidence that hypoxia is a crucial factor for the *in vivo* fungal infection. The study found that *A. fumigatus* did not produce detectable ethanol under normoxic conditions. However, when they were exposed to hypoxia, researchers found significant amounts of ethanol in the shake flask cultures. This may indicate that *A. fumigatus* can ferment glucose or other suitable carbon sources into ethanol in response to hypoxia. Therefore, it can be seen that during fungal pathogenesis, the human fungal pathogens have evolved mechanisms to adapt to grow in a low-oxygen environment.

Human fungal pathogens may be exposed to rapidly changing oxygen availability during fungal pathogenesis (Grahl et al., 2012). This may suggest that fungal virulence may be based on their ability to adapt to hypoxia environment. Also, most of the human fungal pathogens do not live the human body before infections, and the critical question is how those fungi evolved and maintained their ability to adapt to hypoxia. *A. fumigatus* can typically be found in soil or decaying organic material. Those environments are often shown as oxygen-poor areas. It has been found that the oxygen concentration in compost piles can reach approximately 1.5% or even lower (Wang et al., 2007), indicating that organisms that thrive in such area must have evolved hypoxia adaptation mechanisms. In addition, the soil itself could be hypoxic, and the oxygen concentration can be even lower after heavy rains or increased CO₂ levels (Maček et al., 2011). Due to the rapidly changing of oxygen levels, soilborne organisms must have evolved mechanisms of adaptation to hypoxia. Another human-pathogenic yeast, *C. albicans* has been shown that they can grow under anaerobic conditions and ferment glucose into ethanol under such hypoxic conditions, indicating that a Pasteur effect (an inhibiting effect of oxygen on the fermentation process) is associated with other facultative fermentative yeasts (Rozpędowska et al., 2011). In addition, a similar result was also found with a non-pathogenic fungus, *Schizosaccharomyces pombe*, which also evolved mechanisms to adapt to survive in hypoxic conditions (Todd, Stewart, Burg, Hughes, & Espenshade, 2006). Taken together, those observations are suggesting that both human-pathogenic fungi and non-pathogens fungi may have evolved a mechanism which can

make them adapt to hypoxic conditions that occurred during fungal pathogenesis as well as in their natural environments. In other words, hypoxia environments may affect fungi and oomycete growth behaviour during their invasive growth.

Sterol regulatory element-binding proteins in the yeasts *Schizosaccharomyces pombe* (Hughes, Todd, & Espenshade, 2005), and in the filamentous fungus *A. fumigatus* (Willger et al., 2008) have been shown to be important with respect to low oxygen adaptation. Loss of the binding protein, SrbA, can lead to a mutant strain of the fungus, which is incapable of growing in a hypoxic environment. This protein appears to be conserved in filamentous fungi and several yeasts. Also, those regulators in fungi, which proved to be crucial for the adaptation to hypoxia and virulence, can also control sterol and lipid homeostasis in higher eukaryotes and humans (Eberlé, Hegarty, Bossard, Ferré, & Foulfelle, 2004). In ascomycetous fungi, hypoxic adaptation extends well beyond balancing sterol biosynthesis covering energy metabolism and a sophisticated developmental program. However, in *A. fumigatus*, this program can lead to a change of colony morphology (McCormick et al., 2012).

2.1.6 Study invasive growth of hyphae

One way to better understand invasive growth in individual hyphae is to measure the protrusive force and the pressure that they generate. There are a few techniques that have been used to measure turgor pressure in walled cells (Money, 1990). The simplest is the addition of a hyperosmotic solution outside the cell wall. When water leaves the cells, the hyphae plasmolyse. The percentage of plasmolysed cells can be plotted versus the osmolarity of the osmotically active substance in order to yield a measurement of the threshold osmolarity that causes plasmolysis (Money, 1990). However, there are some drawbacks to this technique. For example, scoring for plasmolysis is subjective so that the accuracy of the results may be affected. Another method is using a pressure probe which is a fine glass needle filled with low-viscosity silicone oil. When a cell is impaled with the needle, turgor will force the oil interface into the needle, and the cell turgor can be measured directly (Lew, Levina, Walker, & Garrill, 2004). However, the pressure probe may cause damage to the cell as a consequence of impalement. Methods that can be used for the measurement of protrusive force are different from those for turgor pressure. One

previous study has shown that the magnitude and direction of the protrusive force could be measured by using a lab-on-chip (LOC) platform (Tayagui et al., 2017). With the first use of elastomeric micropillar arrays, force measurements and interaction between hyphae and pillar can be obtained by recording pillar deflection and optical tracking of hyphal widths and extension rates. This study showed a decreased growth rate (tip extension) and an increased tip width during pillar interaction and protrusive force generation. The forces ranging from 0.5 to 10 μN were measured, which were comparable to those generated using other methods (Tayagui et al., 2017). Thus, this platform might be a useful tool for future study in order to further understand the molecular mechanisms that underlie the generation of a protrusive force in particular if that could be combined with a means to control oxygen concentrations.

2.1.7 Fungal infection treatment strategies

As fungal infections are causing widespread population declines in plants and animals, it is critical to investigate their pathogenesis in order to reduce their economic effects and to conserve global biodiversity. A few treatment strategies for pathogenic fungal infections have been considered over the past several years. One of them is focused on the mechanism of hypoxia adaptation. As more and more mechanisms of hypoxia adaptation in human fungal pathogens have been explored, several antifungal compounds which can target fungal proteins that responsible for hypoxic adaptation can be used as an inhibitor for fungal infections (Ernst & Tielker, 2009). Another treatment that has been discussed recently is using hyperbaric oxygen. Hyperbaric oxygen (HBO) was used to treat some infections but not commonly used for pathogenetic fungal infections. Researchers have found a robust HBO-mediated inhibition (over 50%) of *A. fumigatus* biofilm proliferation. However, the effect of HBO under the treatment conditions is transient and fungistatic, suggesting that a novel antifungal drug could be exploited using a drug-HBO combination (Dhingra, Buckey, & Cramer, 2017). For any of these to be realised there needs to be a better understanding of the effects of different oxygen concentrations on invasive growth and an experimental means of controlling these.

2.2 Introduction to microfluidic technology

Microfluidics is defined as the behaviour, manipulation, and accurate control of fluids on the microscale. A lab-on-a-chip (LOC) is a device designed to improve sample preparation, simplify experimental data analysis that used for microfluidics. The commonly used term LOC is also known as the microfluidic chip, or even just the chip.

This section gives a background on microtechnologies used in this research to make LOC device. Technologies, materials to fabricate microfluidic chip are described, along with the oxygen measurement in the chip channel. Parameters which may affect the experiment are discussed.

2.2.1 Applications of the chip

One of the uses of microfluidic devices has been the study of that guide cellular processes (Eisenstein, 2017). Traditionally, such devices were used extensively to measure forces related to mammalian cells (Tyler, 2012). More recently, LOC technology has begun to be adapted for measurements of tip-growing organisms (Stanley, Grossmann, Casadevall i Solvas, & deMello, 2016). This includes the measurement of mechanical forces in fission yeast cells, the study of maze solving and dynamic behaviour of basidiomycetous fungi (Hanson et al., 2006), and the study of contact-induced apical asymmetry in the thigmotropic responses of *Candida albicans* (Thomson et al., 2015). In order to measure protrusive forces, several substrates have been placed in front of an advancing tip, such as waveguide sensors, a calibrated stiffness (e.g. agarose), optical traps or cantilevers. (Bastmeyer et al., 2002; Sanati Nezhad & Geitmann, 2013). Among those techniques, micro-strain gauge cantilevers were likely to be the most suitable method for the measurement of the magnitude of the forces. However, the strain gauge technique also has few drawbacks, such as it can risk underestimating the effective force because of a shape change in the cell with the orthogonal contact of the tip with the flat surface of the sensor. Thus, another approach which can reorient their growth direction in response to a mechanical trigger was developed (Nezhad, Naghavi, Packirisamy, Bhat, & Geitmann, 2013a). A technically more straightforward approach to measure forces exerted by cells during their growth and movement is using elastomeric micropillar arrays (Gupta et al., 2015). They were first developed to study cellular traction forces and later researchers

found that with a few optimisations, these pillar arrays can be adapted for the use of microorganisms (Johari, Nock, Alkaisi, & Wang, 2013). The micropillar-based approach typically combines optical tracking of a pillar top with a simple mechanical model to measure forces. With few modifications, these arrays can be applied to hyphal organisms and provide the capability also to determine the directionality of forces generated (Johari et al., 2013). Using photolithographic miniaturisation approaches, the pillar system can also be used to measure the size of the hyphae in order to study its morphology during invasive growth. Previous work has indicated the suitability of the pillars for force sensing with hyphae (V. Nock, Tayagui, & Garrill, 2015). However, using open arrays of micropillars, only squeezing forces could be recorded, as hyphal tips were observed to preferentially grow into inter-pillar spaces, as opposed to against the sensor pillars. Modified chips were thus developed which confined individual hyphae to narrow channels, which contained single force-sensing pillars. With these LOC platforms hyphae were more likely to grow into pillars, and enabled the magnitude and direction of protrusive force generated by tips of the hyphae to be measured (Tayagui et al., 2017). The protrusive force exerted by hyphae can be measured by the deflection of the pillar tops as the microscope, and the digital camera can record the deflection. Similar to micropillars used in nematodes forces experiment (Gupta et al., 2015), the total force that exerted by hypha is equal to the total deflection of the pillar.

2.2.2 PDMS

The chips are made with polydimethylsiloxane (PDMS), which is a silicon-based organic polymer. The size of surface patterns on PDMS can be down to the nanoscale. PDMS is widely used as it is cheap, and it is simple to reproduce the chip used in the experiments. It is non-toxic to organisms that are grown in the chip. Also, with respect to the current study oxygen and nitrogen can freely diffuse between channels (in the chip used in this study there was a gas channel and a main channel – as described further below) because of their high diffusivity within the PDMS. Additionally, PDMS is transparency which enables continuous visual observation so that high-resolution optical image could be taken. Therefore, PDMS is an ideal material to make chips for this research because of those unique features.

2.2.3 Photolithography

Photolithography is a method that is used to create regular features onto photosensitive material. During photolithography, a light-sensitive layer which is coated on a substrate will be exposed to the UV light in order to transfer a pattern onto the material (Voldman, Gray, & Schmidt, 1999). The process starts with a designed pattern that is made using software and which is then loaded onto a mask writer. A chrome-coated photomask is produced and placed on the top of a coated substrate and exposed to the UV light through the mask. Since the chrome layer is partially removed from the mask, the photoresist will only be exposed to the UV light through the parts where the chrome layer has been removed. There are two types of photoresist, positive or negative. For a negative photoresist, the areas which have been exposed to the UV light will become less soluble. Therefore, once the substrate is immersed in a developer, the areas which have not been exposed to the UV light will be removed, and the pattern will transfer onto the photoresist layer. With positive photoresists, the areas which have been exposed to the UV light are soluble. Hence, after development the exposed areas will be removed, leaving the pattern on the photoresist layer. One of the limitations of this technique is that it requires expensive equipment and clean room conditions. Also, there are only a few types of materials can be patterned using this method so that this technique needs to be combined with other micropatterning techniques to enable the use of a much wider range of materials.

If photolithography is followed by etching, the parts of the substrate which are covered by photoresist will be protected from etching so that the surface of the actual substrate would be etched (Jeon, Simon, & Kim, 2014). After the etching process, the photoresist can be removed by water or organic solvent depending on the resist chemistry.

2.2.4 Soft-lithography

Soft-lithography is another microfabrication technique, which can be used for making patterns on the surface of a polymer. Due to a few limitations of photolithography, the Whitesides group from Harvard University developed this technique to overcome those restrictions (Xia & Whitesides, 1998). It is a parallel patterning method so that it is possible to pattern a large area in a concise period of time. Compared to photolithography, this

technique requires a master replica as an initial master, which is often manufactured by photolithography (Li, Tourovskaia, & Folch, 2003) or some other template-free methods. The master can then be used for moulding a polymer, such as PDMS. One of the advantages of soft-lithography is that it can be used for a broader range of materials than photolithography, such as polymers, ceramics, hybrids, and biomaterials. Another advantage is that this technique does not need a clean room to replicate the patterns so that the technique itself is less expensive. Also, it has the ability to provide resolution down to a few nanometers (Li et al., 2003).

The process starts with a master replica which usually made by using photolithography. Then, a liquid pre-polymer, for instance, PDMS, is poured onto the master and cured, either under room temperature or high temperature to accelerate the process. The cured polymer can then peeled off from the master and baked again to complete curing.

2.2.5 Etching

The etching is a method which can transfer a pattern onto the surface of a material by selectively removing parts of that material by chemical or physical processes. There are three types of etching, drying etching, wet etching, and a combination of both. Dry etching is a method which exposes the surface of a material to the bombardment of ions, while wet etching is to expose the surface of a material to a chemical etchant. In either of these cases, the selective areas of the surface can be masked so that patterns can be transferred onto that surface. Etching can be isotropic, which means that the etching proceeds equally in all directions. Using different material, etching can also be anisotropic, meaning the process only proceeds in one specific direction (Li et al., 2003).

2.3 Oxygen measurement methods

There are several methods that can be used to measure oxygen concentration in a liquid. The three most conventional methods are electron paramagnetic resonance (EPR) oximetry (Diepart, Jordan, & Gallez, 2009), the Clark oxygen electrode, and fluorescent assays.

EPR oximetry uses the resonance of a paramagnetic material to measure oxygen concentration in a liquid, and this method has been shown is suitable for *in vivo* measurement (Diepart et al., 2009). The Clark oxygen electrode uses an oxygen membrane between a cathode and an anode suspended in an electrolyte to measure the oxygen concentration in the liquid (Wu, Yasukawa, Shiku, & Matsue, 2005). When oxygen is consumed, current will be produced at the cathode based on the oxygen levels in the liquid. Also, it can be miniaturised into the chip so that it may be suitable for this research. However, compared to the fluorescence method, it has a lower resolution, and longer response time to the changes in oxygen concentration in the liquid (Grist, Chrostowski, & Cheung, 2010).

Fluorescent measurement of oxygen concentration in the liquid uses a fluorescent probe that can be quenched by oxygen. The emission intensity of the chosen fluorophore is directly proportional to the oxygen concentration in its range of interest. According to quantum mechanics, electrons in atoms can be excited to a higher energy state by absorbing energy from a photon with appropriate frequency. However, the excited energy state is not stable enough so that those electrons will relax back to their ground state after a certain period, and the time of their relaxation is also known as fluorescence lifetime. The energy that lost from those electrons can, therefore, be used as a measurement tool by capturing the emitted photons using a microscope with a suitable filter. Hence, oxygen quenching fluorescence dyes can be used to measure oxygen concentrations. In this research, the more oxygen present in the liquid, the less fluorescent intensity would be measured.

Fluorescence-based measurements are simple, highly sensitive, and have been used in many studies for intracellular oxygen sensing. Thus, in this research, the fluorescent dye ruthenium tris(2,2'-dipyridyl) dichloride hexahydrate (RTDP) was chosen for the measurement of oxygen concentration in the liquid. RTDP is a common soluble oxygen-sensitive dye with high photostability and low toxicity. Several studies have used it to measure the oxygen concentration by merely adding it directly to the media for cell culture (Adler, Polinkovsky, Gutierrez, & Groisman, 2010; Chen et al., 2011; Yang, Luo, Lai, & Ouyang, 2015). The relationship between RTDP fluorescent intensity and dissolved oxygen concentration in the liquid is discussed further in Chapter 3.

Oxygen sensor films embedded into the cell culture substrate is another convenient and straightforward method to measure dissolved oxygen levels in microfluidic chips. They

can be easily incorporated into a LOC device for hypoxia studies (Volker Nock, Alkaisi, & Blaikie, 2010). The novel developed sensor film used solid-state polystyrene (Phillips et al.) based matrix incorporated with an oxygen-sensitive dye, platinum (II) octaethylporphyrin ketone (PtOEPK), following with polyvinylpyrrolidone (PVP) treatment (L. Orcheston-Findlay, Hashemi, Nock, & Garrill, 2018). Since treatments can make the film more suitable for cell-cultures, PVP treated PS/PtOEPK oxygen sensor, which has a stronger cell-substrate adherence, can be used for oxygen measurement for bacteria (Karabanova et al., 2004), cancer cells (L. Orcheston-Findlay et al., 2018), and other compounds (Siddique, Meckel, Stark, & Narayan, 2017), which suggest that those films may not toxic to fungi as well.

PtOEPK can be used as oxygen sensing compound in previous studies because it has high photostability, and sensitive to oxygen, which means it can provide detectable signals for oxygen concentration measurements. PS has been used as the matrix material for a long time (Lerman, Lembong, Muramoto, Gillen, & Fisher, 2018) due to its high oxygen permeability, which oxygen can easily reach to fluorophore by diffusion. Therefore, the PS/PtOEPK matrix/sensor pair could be suitable for this research. However, PS/PtOEPK films can be difficult to be integrated with PDMS channels due to technical issues.

2.3.1 Theory of gas solubility

The concentration of oxygen and nitrogen (solutes) dissolved into the media (solvent) is a key consideration in this research. This means that the physics of solvent and solute interactions must be understood. In general, when a gas contacts a liquid with a specific temperature, some of that gas will passively be dissolved into that liquid. This process stops when equilibrium is reached. The pressure is also needed to be considered as the partial pressure of the free gas also affect the dissolved gas concentration in the solvent at equilibrium. Oxygen solubility in water is followed by Henry's law, which indicates that there is a linear relationship between oxygen solubility and the partial pressure of oxygen. Henry's law constant, k , is specific for oxygen and water (Henry, 1800). One limitation when using Henry's law is that it is only applicable at low concentrations of gas so that when high concentrations of solute are present, Henry's law requires adjustment to take temperature, salinity and solubility into account (Valderrama, Campusano, & Forero, 2016). This means that when working under hypoxia or hyperoxia, adjustments might be needed.

It has been shown that the solubility of oxygen in de-ionised (DI) water is 8.27 mg/L at 25°C at a pressure of 760 mmHg, and in the seawater which has a salinity of 35 g/kg, the solubility drops to 6.60 mg/L at room temperature (Valderrama et al., 2016). This indicates that in this research, the highest concentration of oxygen in the cell culture media is between 6.60 mg/L and 8.27 mg/L at the room temperature. When the oxygen concentration was measured in the main channel, those pieces of information might be supportive.

2.3.2 Gas pressure in the channels

As described in section 2.3.1, it is clear that gas pressure has a linear relationship with gas solubility. In the context of the current study this means that when the pressure in the main channel is high, more oxygen or nitrogen can be dissolved into the media, while if the pressure in the main channel is low, less oxygen or nitrogen can be dissolved in the media. Besides, the pressure in the main channel is partially influenced by the flow controller. In other words, a higher flow rate in the main channel requires more pressure output from the flow controller, leading to higher pressure in the main channel. Moreover, the pressure output from the flow controller is fluctuated over time, which means that the pressure in the main channel might not be constant. Also, the fluctuating pressure in the channel may affect the growth behaviour of tip growth as it may affect turgor pressure in the cell. Therefore, the first part of this research was to find out if the growth behaviour of hyphae was affected by the flow rate of media in the main channel.

The chip used in this research had two gas channels which allow pure oxygen or nitrogen gas to diffuse between the gas channel and the main channel to reach a final equilibrium. Therefore, it was necessary to consider that if the gas pressure may influence their diffusivity in the PDMS. It has been found that at room temperature, the permeability and diffusivity of nitrogen and oxygen were independent of pressure (Singh, Freeman, & Pinnau, 1998; Tremblay, Savard, Vermette, & Paquin, 2006). This suggests that the gas pressure in the gas channel may not have any influences on the oxygen concentration in the main channel.

2.4 Aims of this thesis

The primary aim of this thesis is the development of a LOC device which can control the oxygen level around fungi or oomycetes. This necessitated the design and fabrication of a chip with three channels, one for the growth of the hyphae and two side channels that enabled manipulation of oxygen concentrations in the main growth channel. After fabrication, the chip was used for a preliminary investigation of the growth behaviour of oomycete *Achlya bisexualis* under different oxygen concentrations.

Chapter 3

Methods and Materials

3.1 Design of the chip

The first aim of this research was to develop a LOC device which can control the oxygen concentration inside the chip, and provide an environment for the growth and imaging of hyphae.

Figure 3.1 shows a schematic of the channel geometry on a previously designed chip, which used for the generation of oxygen concentration gradients around cultured cancer cells (Louise Orcheston-Findlay, Hashemi, Garrill, & Nock, 2018). In this chip, each inlet stream has its line of components, oxygen or nitrogen. When two streams are merged at the 3cm long cell-culture channel, an oxygen gradient will be formed. One disadvantage of this chip design is that the oxygen gradient that generated in the channel is not constant. In other words, when fungi or oomycete applied into the channel, they may face a microenvironment where oxygen levels keep shifting at different positions. Hence, a few modifications are required.

In order to create a steady chip microenvironment for hyphae to grow, two additional gas channels were added into the design of the chip as depicted in Figure 3.2. The new chip design has three channels, and each of them has a height of 100 μm . The main channel in the middle was designed for the growth of the hyphae and was about 3 cm long. The media which contain all the nutrients for the growth of the hyphae was designed to come into the main channel through two inlets and flush out via two outlets. The seeding area between two main channel inlets was used for inoculation of the oomycete. Two additional gas channels were designed to fill with either nitrogen or

oxygen in order to generate an oxygen gradient in the main channel. This is possible because PDMS is highly permeable to oxygen. It has been found that the oxygen diffusivity is approximately $4.1 \times 10^{-5} \text{ cm}^2/\text{s}$, and solubility is $0.18 \text{ cm}^3(\text{STP})/\text{cm}^3$ (Mehta et al., 2007). This allows oxygen to passively permeate through the PDMS device. After they reach the equilibrium, the main channel will have a high oxygen concentration area on one side and a low oxygen concentration area on the opposite side. Also, the oxygen gradient that generated in the main channel should be stable after reaching the equilibrium, meaning that all positions in the main channel should have the same oxygen gradient. The optical properties of the chip were such that it enabled both the imaging of hyphae and the measurement of the oxygen gradient generated by two gas channels using a fluorescent dye.

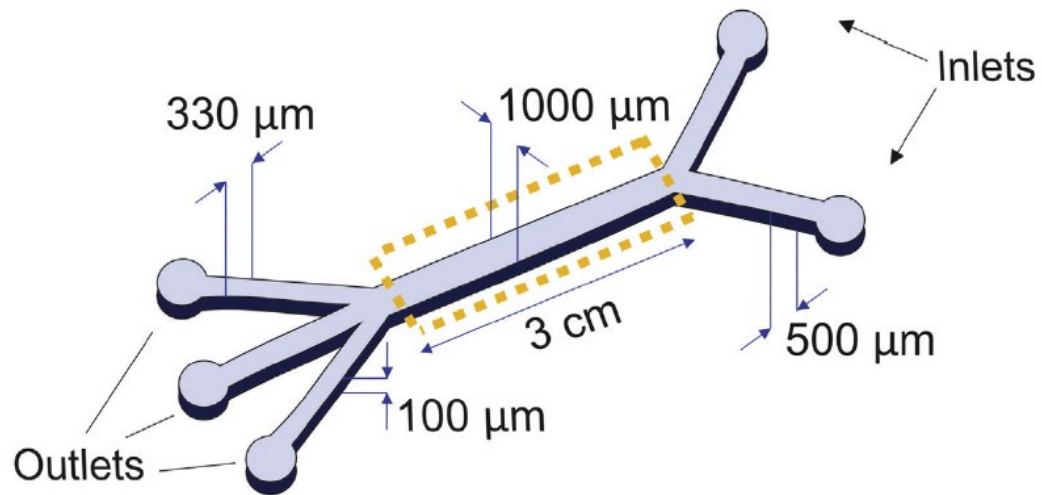


Figure 3.1 A schematic of the channel geometry of the chips used by Orcheston-Findlay et al. (2018) to study the effect of oxygen gradients on cancer cell cultures.

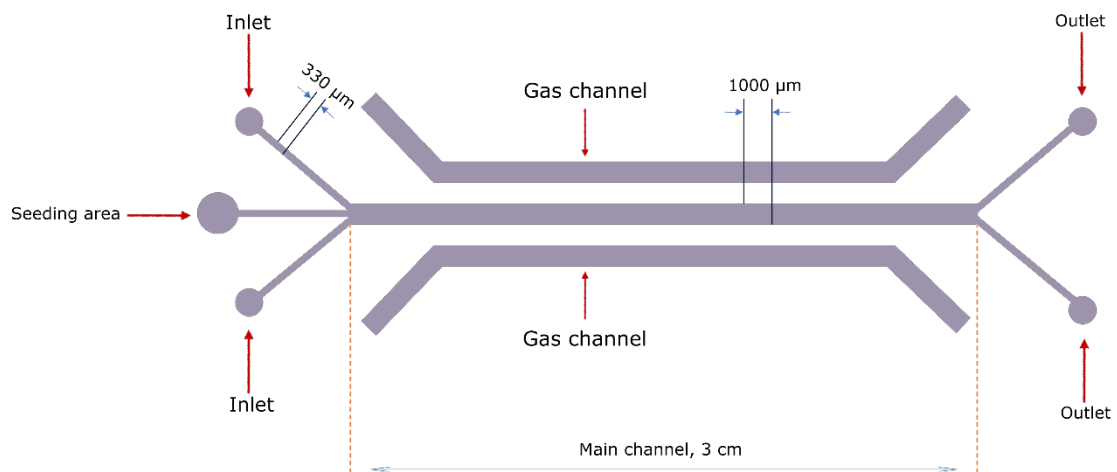


Figure 3.2 A schematic of the newly designed chip. The chip has three channels; each channel has the same height, 100 μm, and same width, 1000 μm. A central channel is used to grow the hyphae while the gas channels are used to control the oxygen concentration in the central growth channel.

3.2 Fabrication of the chip

The manufacture of PDMS chips used in this work was carried out in the microfabrication facility available in the Department of Electrical and Computer Engineering's Nanofabrication laboratory. PDMS chips were prepared using standard photolithography and replica moulding. All channel specification and sizes were firstly designed in L-Edit (Tanner Tools, v15.16) software. The profile was then exported and loaded onto a mask writer (μ PG, 101 Heidelberg) to create a photomask by exposing it onto a blank photoresist plate at a resolution of 400nm. The mask was then developed by an immersion developer (AZ 326 MIF) for 60 seconds and rinsed thoroughly with DI water in order to remove the exposed photoresist. This was followed by drying using a nitrogen gun. The mask was then immersed in a chrome etchant solution (the ratio of ceric ammonium nitrate, perchloric acid, and water was 10.9%, 4.25% and 84.85%, respectively) for another 60 seconds to remove the chrome layer and reveal the mask pattern. Finally, the mask was rinsed with acetone to remove the remaining photoresist layer.

During the process of mask making, a silicon wafer (WaferPro) was dehydrated in an oven at a temperature of 185 °C. After more than 24 hours, the wafer was removed from the oven and then left in room temperature. Cleaning of the wafer was taken in an oxygen plasma asher for 10 minutes at 100W in oxygen (Quorum Emitech, K1050X Plasma Etcher). Because photoresist is susceptible to UV light, fabrication steps were carried out in a clean room with filtered yellow light. While the wafer was in the plasma asher, the laminator (Sky 335R6, DSB) was turned on and set to 30°C. After 10 minutes, the silicon wafer was laminated with a sheet of negative-tone dry film photoresist (SU-8) with a thickness of 100 μ m. The wafer and the mask were then placed in a mask aligner (Karl Suss MA-6 Mask Aligner), and the photoresist layer on the silicon wafer was exposed to 900 mJ/cm² of UV light (365 nm i-line of a mercury lamp) for a specific time in denominations of 10 seconds with an interval of 60 seconds waiting time between each cycle to allow the resist to thermally relax between doses. The lamp intensity and required exposure time was measured and calculated using the lamp test/calculating exposure time procedure on the MA-6 mask aligner working instructions.

The post-exposure bake was taken after 8 hours, during this process the wafer was placed on a programmable hot plate (Alphatech) at 65°C with a 100°C/hour ramp for 5 minutes, and then repeated at 95°C for 10 minutes. The purpose of the two-step ramp between

65 °C and 95°C was to prevent damage of the film with cracks from the high thermal stress in the SU-8 resist. Finally, the wafer was cooled back to room temperature with a ramp of 15°C/hour for 20 minutes which was necessary to reduce film stress and to avoid cracking (Kohlmeier & Gatzen, 2002). The wafer was then left overnight to allow the film to be stabilized. In a 4" non-halogenated solvent, the glass wafer dish was filled with propylene glycol monomethyl ether acetate (PGMEA) and placed into the dish facing downwards for 10 minutes. Therefore, the unexposed areas of the photoresist were then developed. Once developed, the wafer was cleaned with fresh PGMEA and then rinsed with isopropanol alcohol (IPA), acetone, methanol and IPA again. Before moving to the next stage, the wafer was dried out using a low-pressure nitrogen gun.

The steps described above produced a negative master mould. The last step of master mould fabrication was to treat the wafer with vapour trimethylchlorosilane (TMCS, Sigma Aldrich) in a desiccator. This process was done by dropping one drop of TMCS into a small open bottle and placing the bottle in the desiccator with the wafer for 2 hours. A vacuum pump was used to generate a vacuum to help with TMCS evaporation. The coating of TMCS acting as a photoresist layer, which can prevent adhesion between the SU-8 mould and the curing PDMS. Therefore, each mould could be used to produce more microfluidic chips. This surface treatment of the SU-8 mould was taken inside the fume hood as TMCS is a very corrosive compound. A completed mould is shown in Figure 3.3.



Figure 3.3 A completed silicon mould master.

While the silicon wafer was being treated, the liquid PDMS was prepared by pouring and mixing pre-polymer (Dow Corning, SYlgard 184 silicon elastomer base) and the curing agent (Dow Corning, Sylgard 184 curing agent) in a plastic cup at a 10:1 (w/w) ratio. The mixture was then placed in a vacuum desiccator for at least 30 minutes in order to remove any air bubbles that were generated during the mixing. In order to produce a useful, clean PDMS chip, air bubbles in the liquid PDMS must be avoided. Hence, the degassing step was repeated if any air bubbles were still seen in the liquid PDMS. In the meantime, the mould was placed on a clean polyethylene (PE) sheet (OfficeMax, OHP transparency film) followed by a square-shaped flat piece of metal which acted as a stage. The metal stage was applied to help with carrying the wafer. To confine the liquid PDMS during the curing process, a thin metal ring with a diameter 0.5 cm smaller than the wafer was applied and placed on the top of the silicon wafer. The degassed liquid PDMS was then poured onto the wafer, into the ring. A heavy metal weight acting as a lid was placed on the top of the metal ring to prevent the liquid PDMS from leaking out between the ring and the wafer. Figure 3.4 shows the assembly, including the metal stage, the ring, the silicon wafer, the degassed liquid PDMS, and the heavyweight as well as the leakage of PDMS. The whole stack was transferred into a vacuum desiccator for a second degassing process to remove any air bubbles that appeared through dispensing liquid PDMS. The whole assembly was degassed for another 30 minutes to ensure that all air bubbles were removed.

With the help of the metal stage, the stack was placed on a hot plate (Stuart Scientific, SH1D) at 80°C for two hours to cure the PDMS partially. After initial curing, the solid PDMS was detached from the mould by firstly tracing a scalpel (SwannMorton, 3) through the PDMS around the inner surface of the ring and then carefully peeling off the solid PDMS from the mould. The PDMS was then placed between two clean PE sheets and baked again for another 2 hours at 80°C to finish curing. Lastly, the inlet and outlet ports of the main channel and the two gas channels were cut with a 1.2 mm inner diameter handheld dermal punch (ProSciTech, 1.2mm), while the seeding area for inoculation of oomycete was cut with a 3.0 mm inner diameter handheld dermal punch (Elveflow, 3.0mm). Commonly, PDMS microfluidic chips are irreversibly sealed to the glass so that PDMS microchannels can withstand fluid pressure. Therefore, the PDMS was then cut to the correct dimensions for the binding to a microscope glass slide (LabServ, microscope slides).

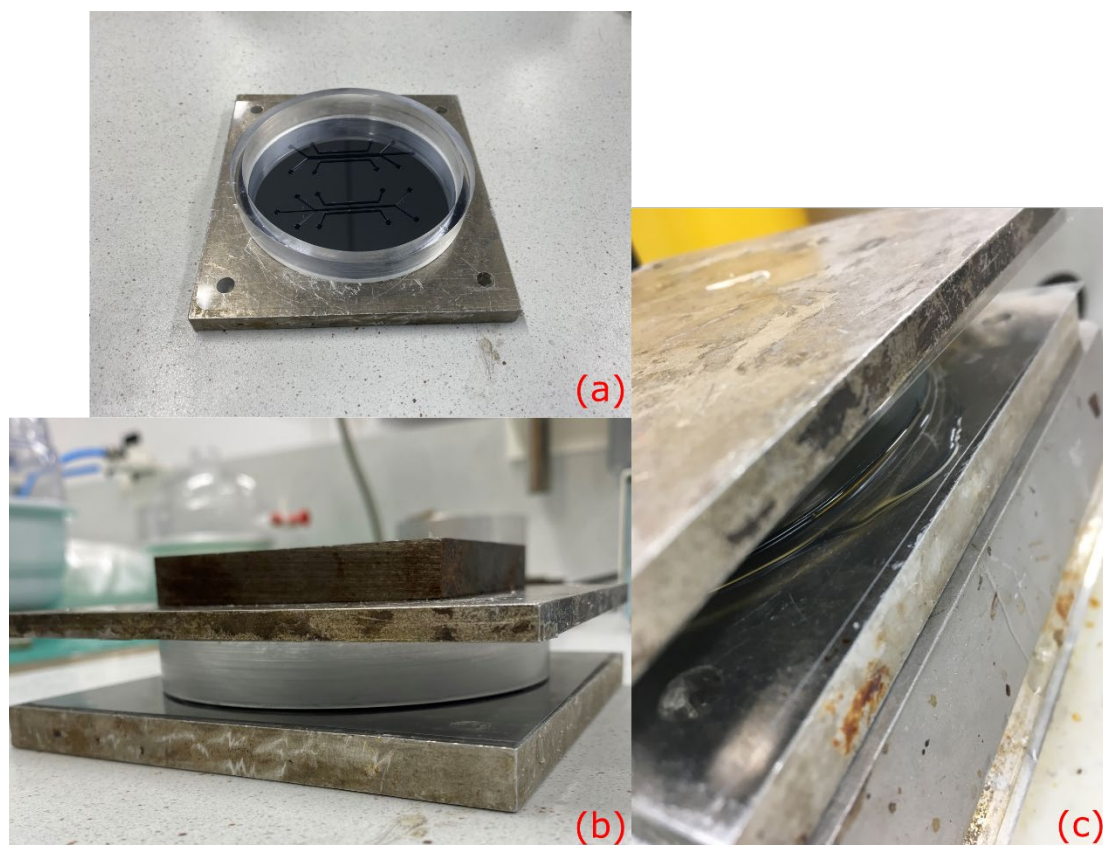


Figure 3.4 Photographs of the setups used for casting PDMS. a) the stack including the metal stage, the PE sheet, the ring, and the wafer; b) PDMS was poured on the wafer within the ring and enclosed with a weight at the top; c) Leaking of PDMS between the ring and the wafer.

In parallel to the casting of PDMS, a plasma cleaner (PIE Scientific Tergeo Plasma Cleaner) was turned on and initialised. Once the machine was vented, the chamber door was removed and placed on the lab bench with the front side of the door upwards to minimise dust falling on the door O-ring. The sample holder was then removed from the chamber and covered with a clean PE sheet to minimise the potential for the PDMS to bond to the sample holder. The sample and a clean microscope glass slide were put onto the middle of the sample holder. The sample holder was carefully placed back into the chamber to start the cleaning process. During the cleaning cycle, the silicon on the surface of both PDMS and microscope glass slide would be activated so that the PDMS could bond to the glass slide by forming a covalent bond with oxygen atoms on their surface. After the cleaning process, the sample and the glass slide was removed from the chamber and

gently contacted together. The assembly was then placed onto a hot plate at 80°C for an additional two hours to ensure the bonding was tightly enough.

The fabricated PDMS chips were placed in a desiccator to be degassed for 2 hours in order to prepare for vacuum-assisted filling. This was because that if the channels on the chip were outgassed, the aqueous solutions could be more quickly filled into the PDMS device and therefore generated no air bubbles in the channel (Monahan, Gewirth, & Nuzzo, 2001). The degassed chip was then sealed into a food-grade vacuum bag using a vacuum sealer (Sunbeam FoodSaver) and stored in the laboratory until use. A completed chip is shown in Figure 3.5.

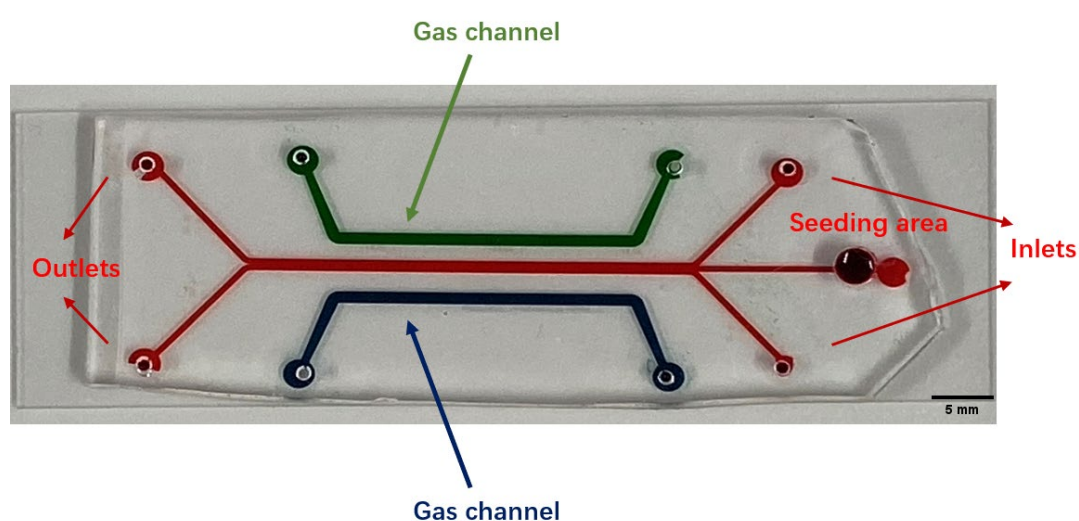


Figure 3.5 A photo of the completed chip that was designed and fabricated for this thesis. To improve visibility the main channel and seeding area were filled with red dye. One gas channel was filled with green dye, while the other gas channel was filled with blue dye.

3.4 Microfluidic experimental setup

Once fabricated the microfluidic chips were incorporated into a larger experimental set up with included flow control and measurement components, the oxygen measurement apparatus and microscope for observations and data collections as depicted in Figure 3.6.

A flow controller (Elveflow, OB1) was used to provide fluid pressure to generate the required flow rate. The flow rate was monitored by flow-through sensors (Elveflow, 2-80

$\mu\text{L}/\text{min}$). Both flow controller and flow sensors were connected to a computer with software (Elveflow SDK, v3) installed. A certain flow rate could be set in the software, and the software would monitor the flow rate that flows through the flow sensor. Every time the current flow rate was read to be higher or lower than the required flow rate, the software would automatically change the pressure output from the flow controller. This feedback loop also has a pair of editable parameters displayed in the software. Those parameters were crucial as they could make the pressure output change faster or slower. To minimise the potential of the cells to react to low rates the lowest values of these parameters were chosen. Due to the limitation of the flow sensor, the flow rate could only be maintained between 2 to 80 $\mu\text{L}/\text{min}$ over extended periods of time.

Rigid and low gas-permeability ethylene tetrafluoroethylene (ETFE) tubing with 1/16" inner diameter (Kinesis, IDEX Health and Science, 1517XL), flanges and connectors (Microfluidic ChipShop), and flow restrictor (Microfluidic ChipShop) were used to connect all the components. Figure 3.6 illustrates how each of these components was set up in the system.

All the experimental components of the microfluidic set up were sent to the autoclave room for sterilisation prior to each experiment. This included the glass bottle of media reservoir, ETFE tubing, flanges and connectors. For those components that could not be sent to the autoclave, such as flow sensors and flow restrictors, they were cleaned using 70% ethanol prior to each experiment.

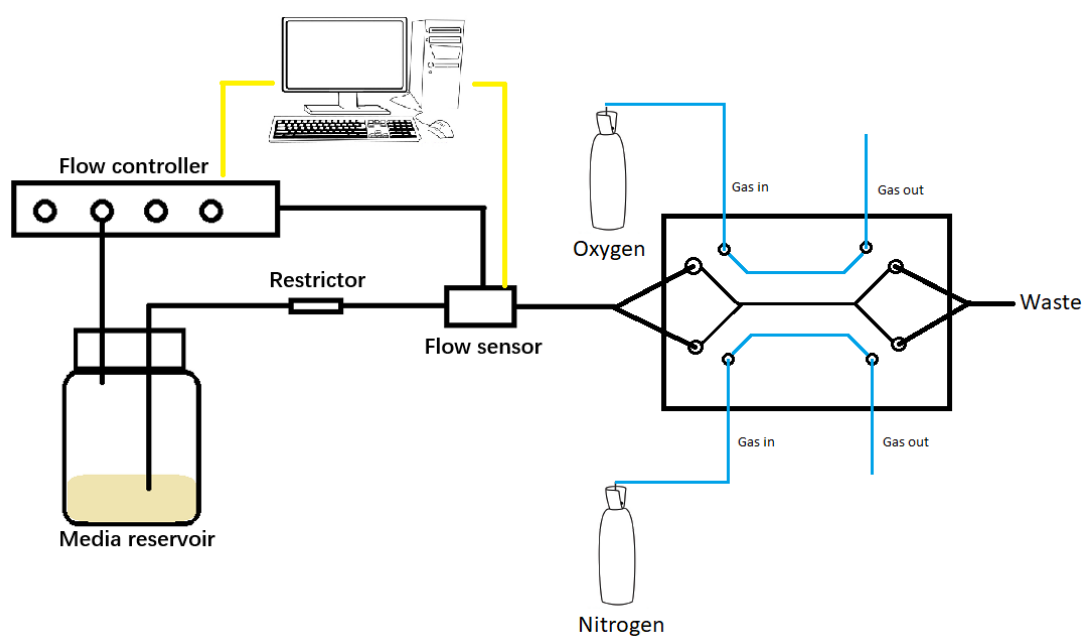


Figure 3.6 The various components that made up the fluidic system and their position in the system. Fluidic connections are solid black, gas are blue, and electrical connections to the computer are shown in yellow.

3.5 Oxygen gradient on the chip

In order to measure the oxygen concentrations in the chip channel, the fluorescent dye, RTDP (Sigma-Aldrich, 1g) was used. Because the concentration of the RTDP and media flow rate could affect the fluorescent intensity of the dye, different concentrations of the RTDP ranging from 0.1 mg/ml to 1.0 mg/ml, and media flow rate were used to find the best dye signal. It has been found that the RTDP signal was best at 1.0 mg/ml and the best media flow rate was 10 μ L/min. Therefore, those two parameters were chosen for further experiments.

RTDP quenching by oxygen is a collisional process. The relationship between fluorescence intensity and dissolved oxygen concentration is described by the Stern-Volmer equation (S. Sun, Ungerböck, & Mayr, 2015):

$$\frac{I_0}{I} = 1 + K_q [O_2] \quad (3.1)$$

or

$$\frac{\tau_0}{\tau} = 1 + K_q [O_2] \quad (3.2)$$

where I_0 or τ_0 is the fluorescent intensity or lifetime without oxygen, I or τ is the intensity or lifetime at the particular oxygen concentration $[O_2]$, and K_q is the Stern-Volmer quenching constant (Sud, Zhong, Beer, & Mycek, 2006). Therefore, from equation 3.1 and 3.2, the concentration of oxygen in the media flow can be calculated either from the fluorescent intensity or lifetime. In this research, oxygen levels were measured using the fluorescent intensity of RTDP as the lifetime measurement requires a piece of specialised equipment that is not available in the laboratory.

3.6 Maintenance of *Achlya bisexualis* cultures

Stock cultures of *Achlya bisexualis* Coker were made using a female strain, which was originally isolated in New Zealand from *Xenopus laevis* dung and obtained from zoospore stores in the University of Canterbury culture collection. Zoospore stocks were stored at -20°C and cultures prepared from zoospores were stored at 4°C . The stock *A. bisexualis* was maintained at room temperature of 25°C on 2% peptone-yeast-glucose (PYG) media.

The 2% PYG media contains 0.125% w/v peptone (Oxoid, UK); 0.125% w/v yeast extract (Oxoid, UK); 0.3% w/v glucose (BDH, UK) and 2% w/v bacteriological agar (Oxoid, UK), made up with distilled water. The organism was sub-cultured every seven days using a 5 mm inner diameter cork-borer and a scalpel. The growing periphery of the colony on the stock plate as chosen for sub-culturing. Then, the cork-borer was used to remove an agar plug from the original agar plate, and the plug was transferred onto the centre of a new agar plate by the scalpel.

3.7 Inoculation of *A. bisexualis* onto the chips

Cultures of *A. bisexualis* were grown on the PYG agar plates for 48 hours at room temperature before inoculation onto the microfluidic chip. An agar plug was taken from the edge of the culture using a handheld dermal punch with 2.5 mm inner diameter (Elveflow, 2.5mm) and transferred to the seeding area of the PDMS chip. As the diameter of the hole was 3 mm, the plug can be slotted into the hole. The agar plug was placed face down in the seeding area so that hyphae were on the bottom. This meant they could grow into the growth chamber and also that when the plugger sealed the port, it did not cause any damage to the hyphae. Prior to inoculation, the chip was filled with PYG broth which contains 0.125% w/v peptone; 0.125% w/v yeast extract; 0.3% w/v glucose (BDH, UK), and made up by distilled water.

3.8 Image collection and processing

All images were taken using a Nikon Eclipse 80i microscope. Images were analysed using ImageJ (version v1.52a).

3.9 Temperature control

The temperature has the ability to affect gas solubility to the media as well as gas diffusivity and permeability in the PDMS (as discussed in Section 2.3.1 and 2.3.2). Therefore, it is crucial to keep the temperature constant during all the experiments. All

experiments were taken at the level 6 PC2 research laboratory which has a temperature control system. The temperature in the laboratory was set up to 25°C at all the time

Chapter 4

Results and Discussion

4.1 Measurement of the Oxygen concentration of the chips

For media flowing at 10 $\mu\text{L}/\text{min}$, the fluorescent signal is taken from the main channel at the start ($t=0$), and the end ($t=60$ minutes) of an experiment is shown in Figure 4.1. As the aim was to investigate hyphal growth behaviour in hypoxia, air and nitrogen gas were chosen to fill the gas channels instead of oxygen and nitrogen gas. This is because air consists of approximately 21% of oxygen which may lead to a broader area under hypoxic in the channel. Theoretically, a stabled oxygen gradient can be formed in less than 10 minutes due to high diffusivity of nitrogen and oxygen in PDMS. However, the data were collected after 60 minutes to make sure that the oxygen gradient was fully formed and stabled.

The concentrations of oxygen in the main channel were then calculated using the Stern-Volmer equation (3.1). A formed oxygen gradient in the channel is shown in Figure 4.1. Position 0 μm indicates the top of the channel which is the closest position to the air-gas channel, while position 1000 μm indicates the bottom of the channel which is the closest position to the nitrogen gas channel. An oxygen gradient formed in the channel in an almost linear manner as shown by the yellow dotted line in the figure. From the Stern-Volmer equation, it shows the relationship between $(I/I_0 - 1)$ and oxygen levels in liquid to be linear which is constant to the calibration. This suggests that the chip design is suitable for the study of hypoxia in relation to hyphal growth.

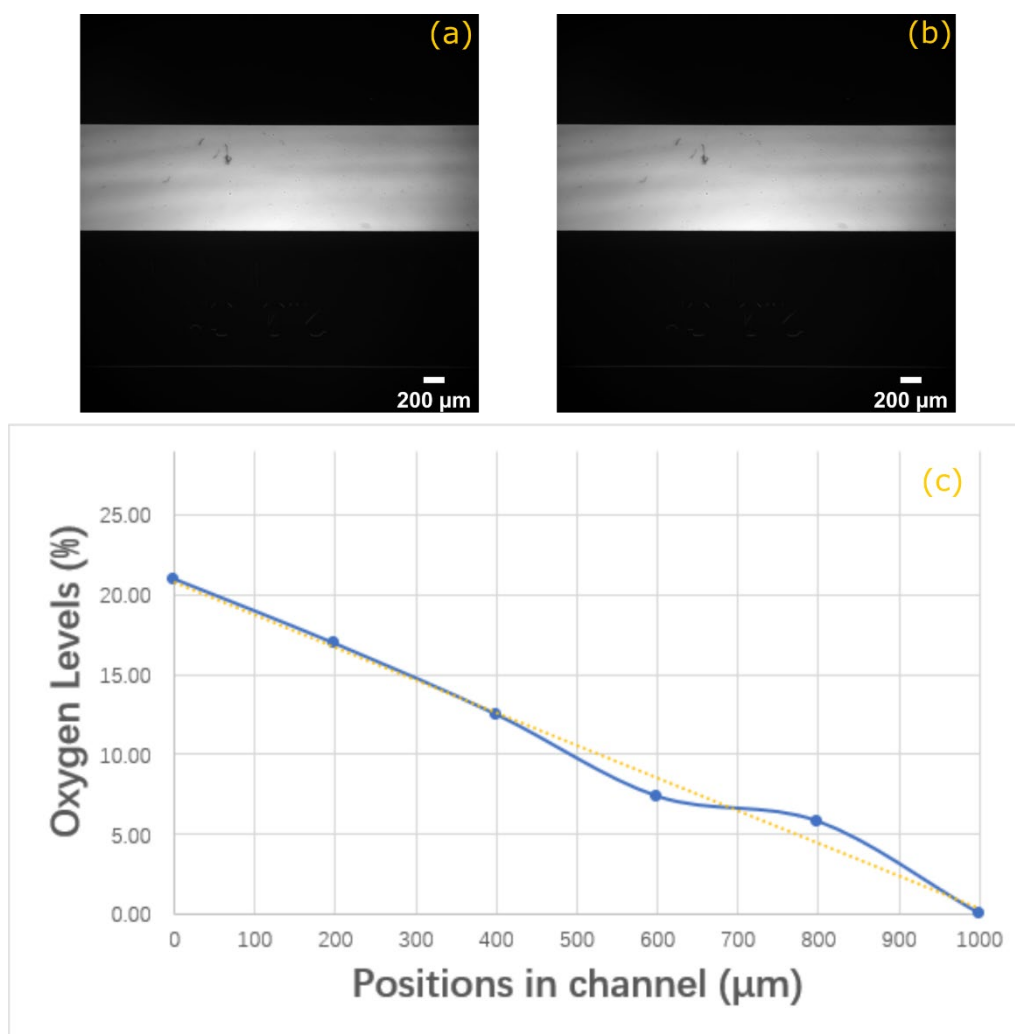


Figure 4.1 Oxygen gradient on the chip. a) The raw signal from the RTDP fluorescent measurement at $t = 0$; b) The raw signal from the RTDP fluorescent measurement at $t = 60$ mins; c) oxygen gradient formed in the channel (black line), and the predicted oxygen gradient in the channel according to the Stern-Volmer equation (yellow dotted).

4.2 Hyphal growth rate against different media flow rate

In order to investigate if the media flow rate could influence the growth behaviour of hyphae, the hyphal growth rate of *A. bisexualis* was measured. Firstly, the growth rates of hyphae from stock cultures were analysed, acting as a baseline for further experiments. To measure the hyphal growth rate, images of the growing edge of the colony on the agar plate were taken every 30 minutes for 5 hours, and ten individual hyphae were marked. The distance the hyphae grew over time was measured and then analysed by software (ImageJ). This experiment was repeated for three times and the data was used to indicate the growth rate of hyphae at zero flow rate. The growth rate of hyphae from a stock culture was $4.98 \pm 0.38 \mu\text{m}/\text{min}$ (mean \pm S.D. (n=30)). This growth rate is slightly slower than previously reports, which were approximately $6 \mu\text{m}/\text{min}$ (Tayagui et al., 2017). However, the growth rates of oomycetes and fungi can be variable, and usually ranging from 1 to $10 \mu\text{m}/\text{min}$ (McKerracher & Heath, 1987). Therefore, the growth rate of *A. bisexualis* hyphae on PYG agar plate may be altered due to temperature, pressure or other factors, but the results are still acceptable.

When inoculated onto the chips, a large number of *A. bisexualis* hyphae started to grow from the seeding area into the growth chamber after approximately 5 hours. Images were started to be taken when at least ten hyphal tips had grown into the main channel. The distance of the hyphal tip travelled between each time interval was measured and analysed. The media flow rate in the main channel was set as $5 \mu\text{L}/\text{min}$, $10 \mu\text{L}/\text{min}$, $15 \mu\text{L}/\text{min}$, $20 \mu\text{L}/\text{min}$ or $30 \mu\text{L}/\text{min}$, and for each flow rate experiments were repeated three times. The growth rate of hyphae against different media flow rates is shown in Figure 4.2.

Compared to a previous study, the growth rates of the isolate of *A. bisexualis* hyphae in microfluidic chips are ranging from $6\text{--}8 \mu\text{m}/\text{min}$, the growth rate of hyphae in this research was lower (Muralidhar et al., 2016). However, it can be seen from the graph that there have no significant changes (T-test, $P > 0.05$) in growth rate when different media flow rates were applied and as such media flow rate in the main channel has no effect on the hyphal growth rate.

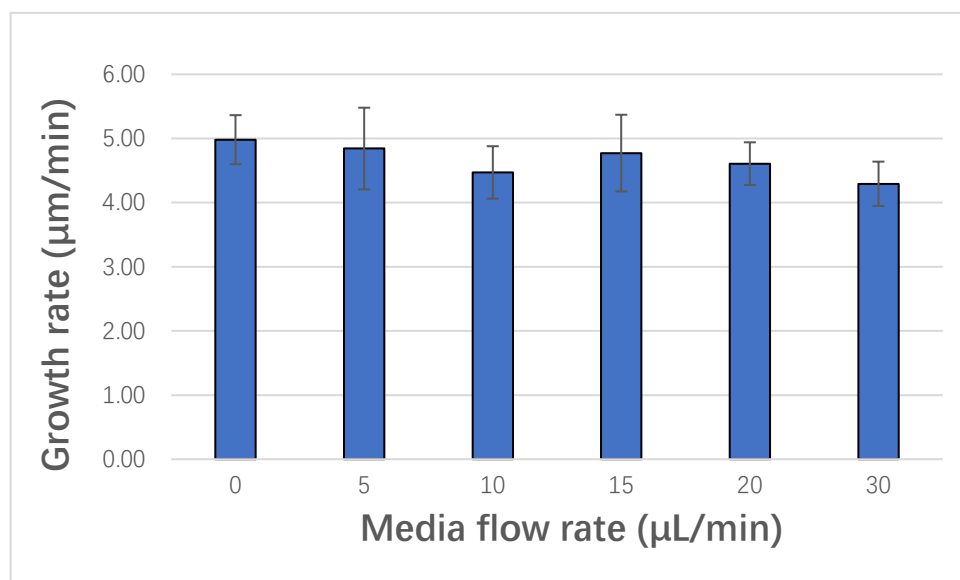


Figure 4.2 Hyphae growth rate at different media flow rates. There was no significant effect on growth rate at the different flow rates.

4.3 Hyphal diameter in different media flow rate

To further confirm that the media flow rate has no influences on the growth behaviour of hyphae, the diameters of hyphae that were growing in the channel was monitored and analysed. As unhealthy or stressed hyphae often show changes in the tip and hyphal morphology, so the diameter of hyphae can be used as an indicator of their state of health. Similar to the growth rate measurement, the diameters of ten selected hyphae from stock cultures were analysed first to set up a baseline for further experiments. Images were taken every 30 minutes for 5 hours, and hyphal diameter was measured about 100 μm behind the tips. The diameter of hyphae from the stock culture was $26.8 \pm 2.55 \mu\text{m}$ (mean \pm S.D. ($n=30$)). These results are comparable to those measured on PYG agar plates in a previous study (Tayagui et al., 2017). The diameters of hyphae in the main channel were then measured on the chips at different media flow rates (5 $\mu\text{L}/\text{min}$, 10 $\mu\text{L}/\text{min}$, 15 $\mu\text{L}/\text{min}$, 20 $\mu\text{L}/\text{min}$ and 30 $\mu\text{L}/\text{min}$) and each diameter measurement experiments were repeated for three times. Results of the diameter of hyphae against different media flow rate are shown in Figure 4.3.

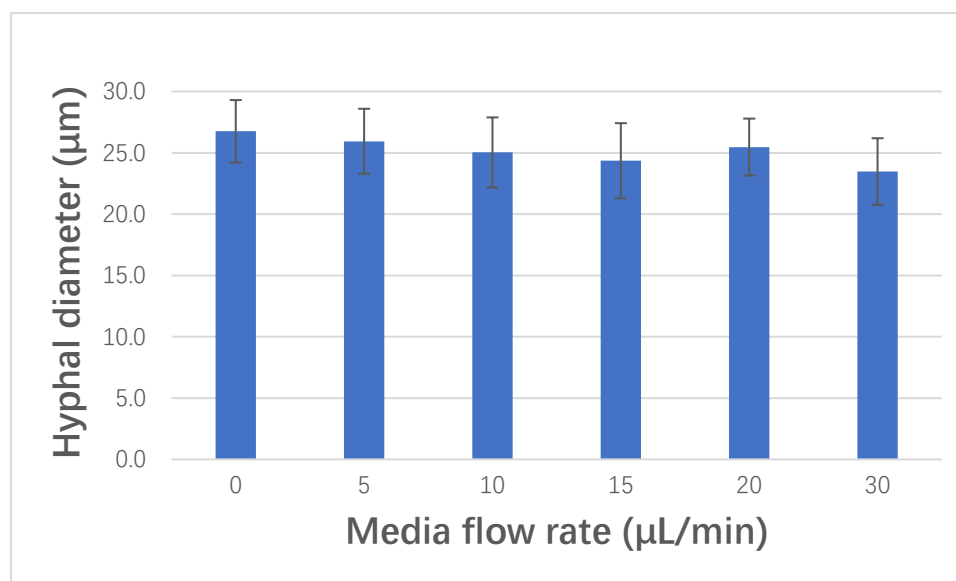


Figure 4.3 The effect of different media flow rates on hyphal diameter. The diameter was measured 100 μm behind the hyphae tips. Flow rate had no significant effect on diameter.

The media flow rate has no significant (T-test, $P > 0.05$) influence on hyphal diameter. However, some researchers have reported that the diameter of hyphae might be affected by the channel parameter as hyphae might become thinner than usual when they grow in a thin channel construction (Nezhad, Naghavi, Packirisamy, Bhat, & Geitmann, 2013b).

For the most part hyphae were observed to grow in a linear manner in the main growth channel without deviations (Figure 4.4). Moreover, the typical characteristics of tip growth were observed in the experiment, such as the forward movement of bulk cytoplasm at the hyphal tip, and the retrograde movement of small refractile vesicles. Combined with the results of the diameter of hyphae in different media flow rate, it can be seen that hyphae in the channels appeared healthy. Therefore, the media flow rates, or the changes of pressure in the main channel, have no effect on the hyphal growth behaviour.



Figure 4.4 Hyphae growing straight in the channel at a flow rate of 30 $\mu\text{L}/\text{min}$. Time interval of each images was approximately 60 minutes.

4.4 Hyphal growth behaviour in hypoxia

Hyphae of *A. bisexualis* were inoculated and grown in the main channel of the chip at a media flow rate of 10 $\mu\text{m}/\text{min}$. The flow rate was controlled by the flow controller and monitored by the flow sensor. The initial images of hyphae were obtained using a Nikon Eclipse 80i microscope at low magnification. Hyphae had grown into the main channel after approximately 8 hours of inoculation. Ten hyphae were selected, and their growth rate and diameter were measured. Similar to the previous experiments of growth rate measurement, ten hyphae were grown at a rate of $4.51 \pm 0.53 \mu\text{m}/\text{min}$ (mean + S.D. (n=10)). The diameter of hyphae, which was measured 100 μm behind the tip, was shown that hyphae were grown healthy in the channel. The diameter was $24.1 \pm 2.33 \mu\text{m}$ (mean + S.D. (n=10)) which is consistent with the previous experiments.

Nitrogen gas and air were applied to the gas channels to generate an oxygen gradient in the main channel. As this research was mainly focused on the hyphal growth behaviour under hypoxic conditions, the air, which consists of approximately 21% of oxygen, was applied. Images were taken every 5 minutes for 1 hour immediately after the gas was applied, and every 30 minutes until the experiment finished. Also, the growth rate and diameter of hyphae in the channel were measured after the oxygen gradient was generated. Data shows that hyphae were grown in hypoxic condition at a rate of $4.94 \pm 0.71 \mu\text{m}/\text{min}$ (mean + S.D. (n=10)) which was slightly faster than normoxic conditions. The diameter of the hyphae in hypoxia was $24.7 \pm 2.62 \mu\text{m}$ (mean + S.D. (n=10)), which is comparable to previous experiments.

From the data of the growth rate and diameter of hyphae under hypoxic conditions, it suggests that all hyphae in hypoxia were not unhealthy or stressed. Hyphae in hypoxia grow slightly faster than those grown in normoxic (atmosphere) conditions which may suggest that more protrusive force might be extracted from them. In other words, hyphae in hypoxic conditions may be more aggressive than those who grow in the atmosphere as they can generate greater force to penetrate through solid media surrounding them.

In addition, the growth direction of hyphae in the main channel was monitored. From the observation of the previous experiments, and as discussed in section 4.3, it suggests that the hyphae were more likely to grow straight in the main channel. However, their growth behaviour changed significantly when those hyphae were growing in the channel with an oxygen gradient. From Figure 4.5, it can be seen that some hyphae, which were grown in

a high oxygen concentration area, changed their growth direction towards the hypoxic area. The majority of them altered their growth directions at approximately 30°, and few of them even had an over 90° direction change. This suggests that *A. bisexualis* hyphae were more likely to grow towards hypoxic conditions.

A previous study from our lab has shown that hyphae may have the ability to reorient their growth path to avoid barriers (V. Nock et al., 2015). A similar observation has also been made by the dimorphic yeast *C. albicans*. It is likely that they can sense the geometry of the channel and altered their growth based on the design of the channels on the PDMS chips (Thomson et al., 2015). Those suggest that if there were sufficient space in front of hyphae, they would not change their growth directions. Due to the main channel geometry of the chip used in this research, all hyphae were grown straight and barely altered their growth directions. Similar to their ability to avoid barriers in their growth path, *A. bisexualis* might also have the ability to sense the surrounding oxygen concentration. However, some of the hyphae were still grown straight after oxygen gradient was applied. Therefore, the mechanisms of when and why *A. bisexualis* hyphae altered their growth behaviour in an area of interest to investigate in the future.

We also compared the hyphal growth behaviour before and after the oxygen gradient had formed in the channel. Figure 4.6 shows the growth behaviour of hyphae in the same experiment. Under the same experimental conditions, most of the hyphae were growing straight before nitrogen and air were applied to the channel, while hyphae started to alter their growth direction after the oxygen gradient formed and stabilised in the channel. Particularly, the average of growth direction changes before oxygen gradient applied was $14.36 + 11.73^\circ$ (mean + S.D. (n=15)), while the average of growth direction changes after oxygen gradient applied was $79.21 + 40.23^\circ$ (mean + S.D. (n=15)). This shows a significant changes in their growth directions (T-test, $P < 0.05$), and further indicates that hyphae behave differently after the oxygen gradient was applied in the channel.

The presence of a gradient in the channel might not be necessarily indicative of insufficient oxygen transport to the cells. However, it is essential to understand and characterize the gradients generated in the channel could influence hyphal responses in the microfluidic chip.

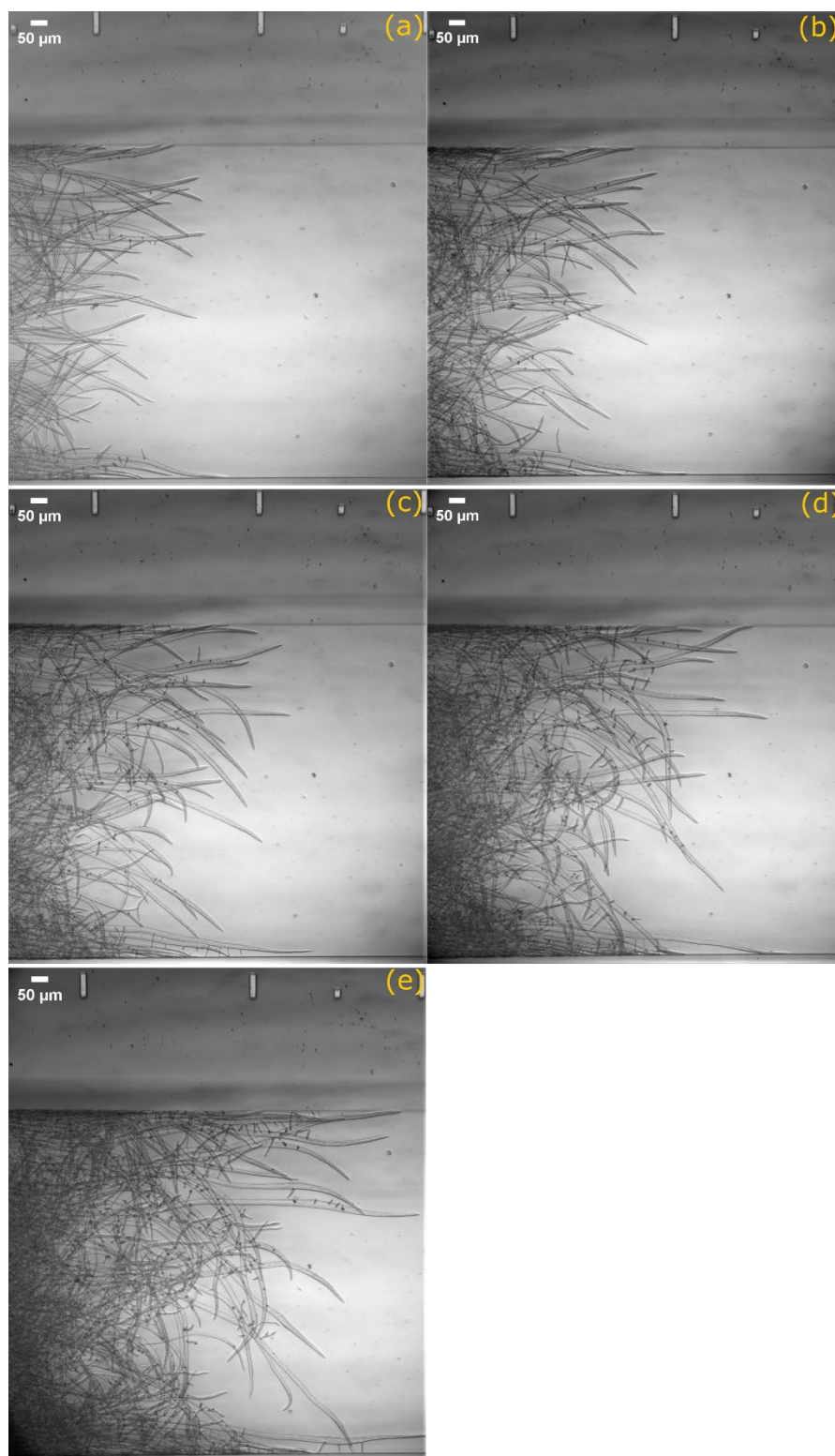


Figure 4.5 The growth behaviour of hyphae toward the more hypoxic environment. In the Figure the upper part of the channel had high oxygen and the bottom part of the channel had low oxygen. Image (a) to (e) were taken at time 0, 30, 60, 90, 120 minutes, respectively.

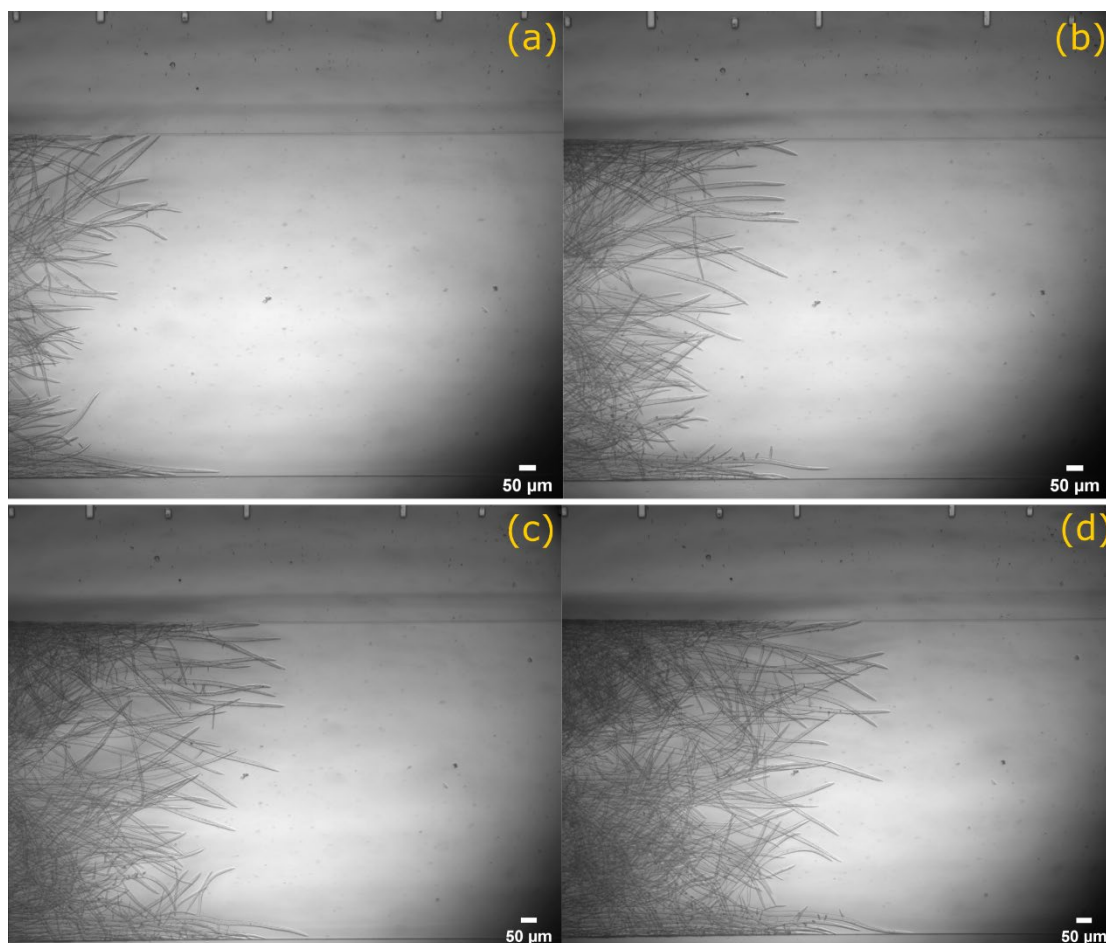


Figure 4.6 The growth behaviour of hyphae in the normoxic environment. Image (a) to (d) were taken at time 0, 30, 60, 90 minutes, respectively.

4.5 Experiment Issues

There were several issues that arose in this research. In this section, those issues are described, and some possible solutions to overcome them are discussed.

Air bubbles

For many researchers studying microfluidics, bubbles have always been an issue that limited the data collection or invalidated the whole experiment. The basis of the design of the chip used in this research is that PDMS has a high oxygen and nitrogen permeability. Therefore, when pure oxygen and nitrogen were applied to the gas channels, they could freely diffuse between the channels. However, this property of PDMS can also lead to the generation of air bubbles in the channel.

In this research, air bubbles in the channel will not only affect oxygen concentration measurements but also able to affect hyphal growth. Since RTDP can only be dissolved in liquid, when an air bubble formed during the process of RTDP fluorescent measurement, the entire area would be shown as completely black under the microscope and so no data could be collected from that area. As previously discussed, hyphae were likely to have the ability to avoid any barrier in their growth path and tend to avoid air bubbles. Also, there were still few hyphae been found to grow straight into the air bubbles on their growth path. This may be because the air bubble is big enough and almost block the channel. Under this circumstance, most of the hyphae would choose to grow into the air bubble, leading to death eventually due to the limitation of nutrients. Figure 4.7 shows the effects of air bubbles during an experiment. After an oxygen gradient was formed in the channel, all hyphae were forced to grow at one side of the channel (at this time the normoxic side) due to the generation of air bubbles. Therefore, in this case, the observation of hyphal growth behaviour in different oxygen levels was not possible.

Air bubbles can also affect media flow, causing a high fluctuation of flow rate when an air bubble formed in the connecting tubing. Since the tubing is narrow, it would be challenging to flush them out so that they could block a large area. That would signal the flow controller to increase the pressure to maintain the flow rate in the channel. The increased pressure could lead to shrinkage of the air bubble, and cause a significant increase in flow rate. Increase in flow rate would then signal the flow controller to decrease the pressure, leading to a swell of the air bubble, causing a decrease in flow

rate. Thus, a cycle begins, causing a fluctuation of flow rate due to the generation of the air bubbles.

One way to get rid of air bubbles was to increase the pressure provided from the flow controller to its limit (usually 1000 mbar). With that high pressure, the flow rate would increase to a high level, and air bubbles could at times be flashed out of the channel although the success rate in removing bubbles in this manner was low.

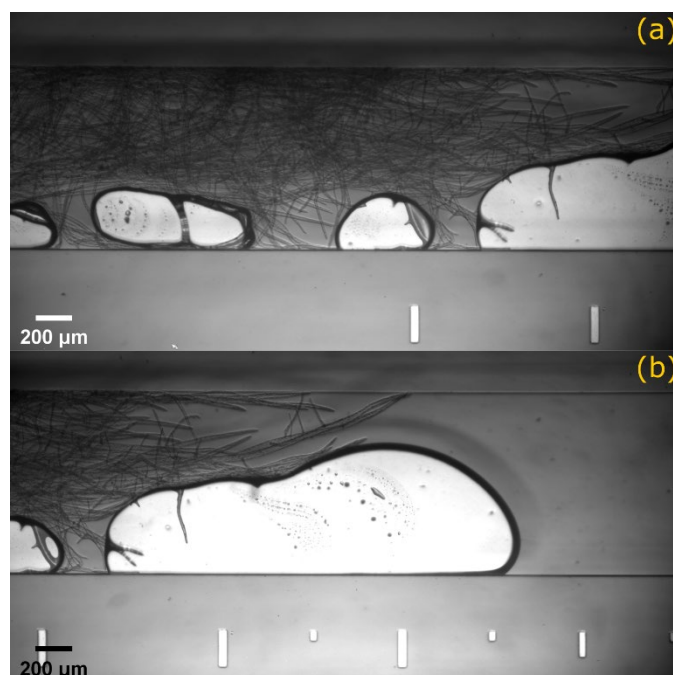


Figure 4.7 The effects of the formation of air bubbles on hyphal growth behaviour. Images were taken at a) the back; b) the front of the hyphal growth in the same experiment and the same time.

Hyphal growth in the channel

In some experiments the number of hyphae growing in the channel was so large this would lead to a blockage of the channel, stop the media flow, generate air bubbles, and cause the eventual death of hyphae. Thus, the seeding area was punched as close to the main channel entrance as possible to overcome this issue. Since data collection started when hyphae reached to the main channel, this would save some time before hyphae entirely blocked the channel. Also, images for measurement of hyphal growth rate and diameters were taken at the front side instead of the back side due to the same issue.

RTDP issues

RTDP has been used in many studies as an oxygen measurement tool simply by adding it directly to cell-culture media (Adler et al., 2010; Ayyash, Wu, & Ravi Selvaganapathy; Mehta et al., 2007; W. Sun et al., 2018). Those cell cultures include cancer cells, mouse myoblasts, and *E.coli*, which suggest that RTDP is not cytotoxic to most of the cells. However, some studies have suggested that mammalian cells might be affected by RTDP due to its cytotoxic and phototoxic effects (Dobrucki, 2001). Conversely other have shown that the presence of a high concentration of RTDP (1.0 mg/mL) in the media would only result in less than 10% of cells dying after 5 hours exposure to the dye (Mehta et al., 2007).

In this research, a high concentration of RTDP (1.0 mg/mL) was used to get good fluorescence signals. However, as shown in Figure 4.8, when RTDP was added to the media, all hyphae stopped their growth due to the dissolved RTDP in the media flow. The experiment was continued for an additional 2 hours to confirm this phenomenon. This observation indicates that a high concentration of RTDP may be cytotoxic to hyphal cells. Therefore, a series of experiments was taken to find out a safe concentration of RTDP for hyphae to survive. It has been found that when the concentration of RTDP was lower than 0.02 mg/mL, this did not affect hyphal growth. However, with that concentration, the fluorescence signal became undetectable. This indicates that real-time oxygen concentration measurement may not be able to work in this research.

To solve this issue, the oxygen concentration in the channel was measured first, and then media with RTDP was flashed out of the channel, followed by immediate inoculation of hyphae. All experimental conditions, including temperature, pressure, and flow rate were maintained the same before and after the inoculation.

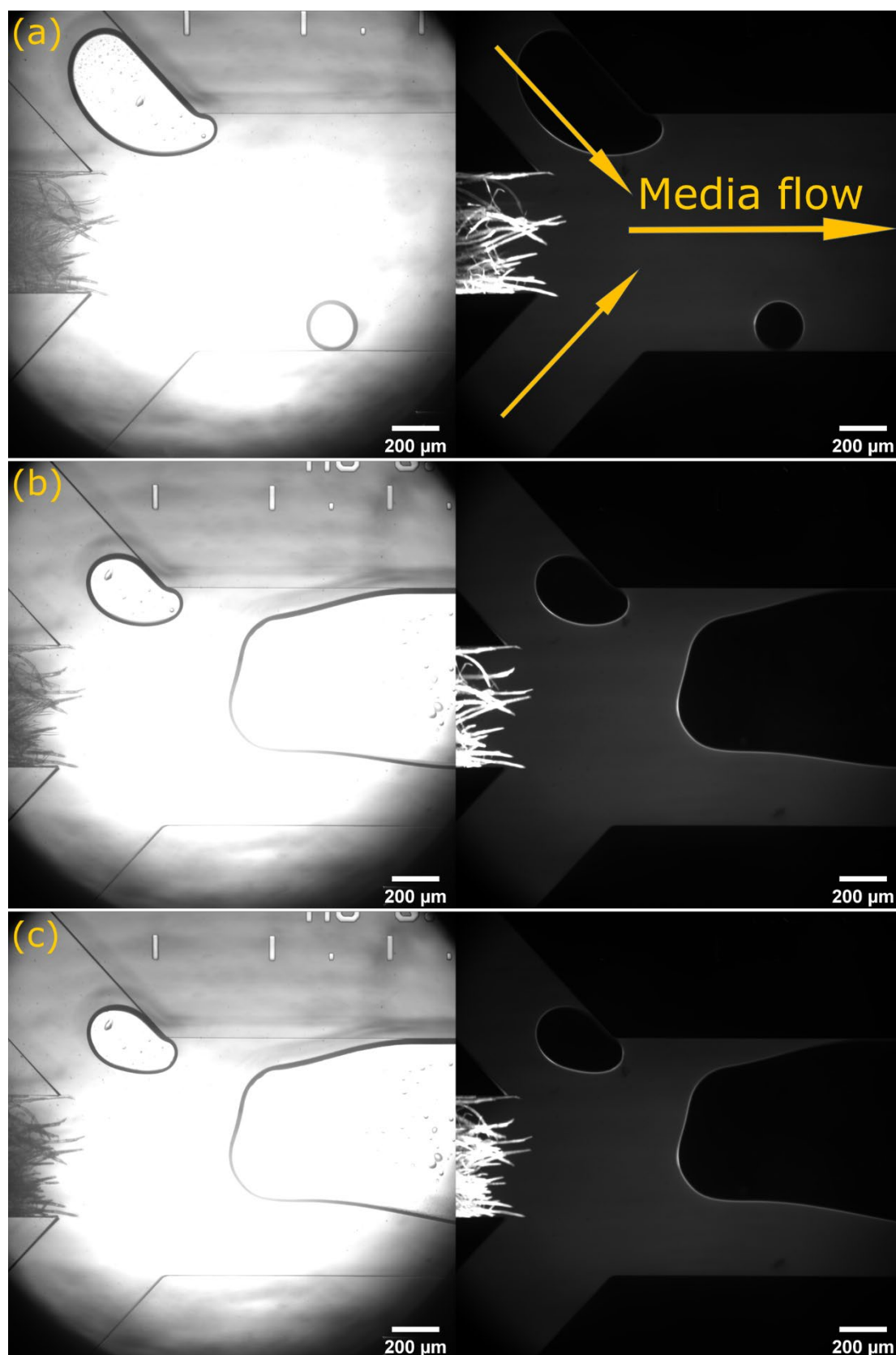


Figure 4.8 Hyphae stopped growing at the entrance of the main channel due to the RTDP in the media flow. a) microscopic and fluorescent images were taken at $t = 0$; b) microscopic and fluorescent images were taken at $t = 60$ minutes; c) microscopic and fluorescent images were taken at $t = 120$ minutes. 49

Chapter 5

Thesis Conclusion and Future Work

5.1 Thesis summary and conclusion

Fungi and oomycetes are a worldwide threat to both animals and plants. It has been suggested that oxygen level during fungal pathogenesis is an essential factor. Also, fungi are thought to be confronted with low levels of atmospheric oxygen during their infections. Therefore, tip growth, which is the process by which fungi and oomycetes grow, could be affected by cellular oxygen concentration. This suggests that cyclic hypoxia may affect their invasive and pathogenic capabilities.

The work described in this thesis contributes to the field by the development of a lab-on-a-chip device which can control the oxygen environment during hyphae invasive growth, and therefore provide an opportunity to observe hyphal growth behaviour during tip growth. Also, the system that was designed and used in the experiment has an off-chip oxygen concentration control so that it can mimic the *in vivo* microenvironment.

The chip that was designed in this research was made by PDMS, and had three channels on it. One main channel used for hyphae growth, along with two gas channels that were filled with either air or nitrogen for the generation of oxygen gradient in the main channel. After application of air and nitrogen to the gas channel, the fluorescent intensity of RTDP in the channel could be measured. The oxygen concentration in the media was calculated using the Stern-Volmer equation based on the fluorescent intensity data. The result showed an almost linear oxygen gradient was formed in the channel, which matches previous studies (Mehta et al., 2007). This suggests that the chip could be used for the investigation of the invasive capability of hyphae in hypoxic conditions. In addition, it is noted that if pure oxygen gas was used in the gas channel instead of air, the oxygen

tension could be elevated to over 70% in theory. This is to say, the chip that designed in this research can not only be used for hypoxia studies, but also hyperoxia studies.

The system used in this research to control the flow rate and oxygen concentration in the channel was efficient, easy to set up, and maintenance. Thus, it can be used for future studies as well as any other relative studies.

In order to show the applicability of this device, the oomycete *Achlya bisexualis* was inoculated on the chip. Since the media flow rate might affect the growth behaviour of hyphae due to the changes of pressure in the channel, hyphae growth rate at different media flow rate was measured and analysed. The results indicate that the differences between flow rate have no effects on hyphal growth rate. Hyphal diameters were also measured in the experiments, which suggest that all hyphae were growing healthily in the channel, and were not affected by altered media flows.

An oxygen gradient can be formed in the channel when air and nitrogen were applied in the two gas channels. From the fluorescent intensity data, the oxygen concentration of any locations in the channel could be calculated. When *A. bisexualis* was inoculated on the chip, a different growth behaviour was observed. Before the oxygen gradient was applied to the chip, most of the hyphae were observed to grow straight, parallel to the axis of the channel, however, after an oxygen gradient formed in the channel, some of the hyphae deviated from the high oxygen area and grew towards the low oxygen area. This might suggest that hyphae of *A. bisexualis* were more likely to grow in a lower oxygen concentration.

With the LOC device developed in this work, an oxygen gradient was successfully generated when hyphae were grown in the channel. The presence of this oxygen gradient might not be undoubtedly indicative of insufficient oxygen transport to the hyphal cells. However, it is still essential to understand and characterize the gradients generated in the channel could influence hyphal responses in the microfluidic chip. Also, it is noted that this oxygen gradients of the type described in this work have not previously been demonstrated for hyphal growth behaviour studies in continuously perfused PDMS microdevices.

5.2 Future work

It is unfortunate that real-time oxygen measurement in the channel was not possible when hyphae were growing in the channels due to the high concentration of RTDP needed to provide a detectable fluorescent signal, which was cytotoxic to the hypha. Therefore, in the future, additional fluorescent dyes could be tested to see if concurrent growth and oxygen level measurements are possible. In addition, the measurement of oxygen concentrations inside the hyphae could also become possible. Therefore, a better understanding of hyphal growth behaviour at different oxygen levels could be generated.

Although many studies suggested that hypoxia may enable hyphae to grow invasively, the molecular mechanisms underlying this is still unclear. A previous study had used micropillars on the chip to measure the protrusive force generated from individual hyphae (Tayagui et al., 2017). Based on the findings from this research, a few modifications could be made to this oxygen controlled device. With the newly designed chip, it may be possible to measure the protrusive force of individual hyphae in an oxygen controlled environment, and that would fill more gaps in understanding the relationship between the invasive capability of hyphae and oxygen levels.

Reference

- Adler, M., Polinkovsky, M., Gutierrez, E., & Groisman, A. (2010). Generation of oxygen gradients with arbitrary shapes in a microfluidic device. *Lab Chip*, 10(3), 388-391. doi:10.1039/B920401F
- Ayyash, S., Wu, W.-I., & Ravi Selvaganapathy, P. (2014). *Fast and inexpensive detection of bacterial viability and drug resistance through metabolic monitoring*.
- Bastmeyer, M., Deising, H. B., & Bechinger, C. (2002). FORCE EXERTION IN FUNGAL INFECTION. *Annual Review of Biophysics and Biomolecular Structure*, 31(1), 321-341. doi:10.1146/annurev.biophys.31.091701.170951
- Blackwell, M. (2011). The Fungi: 1, 2, 3 . 5.1 million species? In (Vol. 98, pp. 426-438). United States: Botanical Society of America.
- Blehert, D. S., Hicks, A. C., Behr, M., Meteyer, C. U., Berlowski-Zier, B. M., Buckles, E. L., . . . Stone, W. B. (2009). Bat White-Nose Syndrome: An Emerging Fungal Pathogen? *Science*, 323(5911), 227-227. doi:10.1126/science.1163874
- Cameron, S. A., Lozier, J. D., Strange, J. P., Koch, J. B., Cordes, N., Solter, L. F., . . . Robinson, G. E. (2011). Patterns of widespread decline in North American bumble bees. *Proceedings of the National Academy of Sciences of the United States of America*, 108(2), 662-667. doi:10.1073/pnas.1014743108
- Chang, Q., Jurisica, I., Do, T., & Hedley, D. W. (2011). Hypoxia predicts aggressive growth and spontaneous metastasis formation from orthotopically grown primary xenografts of human pancreatic cancer. *Cancer research*, 71(8), 3110-3120. doi:10.1158/0008-5472.CAN-10-4049
- Chen, Y.-A., King, A. D., Shih, H.-C., Peng, C.-C., Wu, C.-Y., Liao, W.-H., & Tung, Y.-C. (2011). Generation of oxygen gradients in microfluidic devices for cell culture using spatially confined chemical reactions. *Lab on a chip*, 11(21), 3626. doi:10.1039/c1lc20325h
- Dhingra, S., Buckey, J. C., & Cramer, R. A. (2017). Hyperbaric Oxygen Reduces Aspergillus fumigatus Proliferation In Vitro and Influences In Vivo Disease Outcomes. *Antimicrobial Agents and Chemotherapy*, 62(3). doi:10.1128/AAC.01953-17
- Diepart, C., Jordan, B. F., & Gallez, B. (2009). A New EPR oximetry protocol to estimate the tissue oxygen consumption in vivo. *Radiation research*, 172(2), 220.

- Dobrucki, J. W. (2001). Interaction of oxygen-sensitive luminescent probes Ru(phen)₃²⁺ and Ru(bipy)₃²⁺ with animal and plant cells in vitro : Mechanism of phototoxicity and conditions for non-invasive oxygen measurements. *Journal of Photochemistry & Photobiology, B: Biology*, *65*(2), 136-144. doi:10.1016/S1011-1344(01)00257-3
- Eberlé, D., Hegarty, B., Bossard, P., Ferré, P., & Foulfelle, F. (2004). SREBP transcription factors: master regulators of lipid homeostasis. *Biochimie*, *86*(11), 839-848. doi:10.1016/j.biochi.2004.09.018
- Eisenstein, M. (2017). Mechanobiology: A measure of molecular muscle. *Nature*, *544*(7649), 255-257. doi:10.1038/544255a
- Ernst, J. F., & Tielker, D. (2009). Responses to hypoxia in fungal pathogens. *Cellular Microbiology*, *11*(2), 183-190. doi:10.1111/j.1462-5822.2008.01259.x
- Evans, H. C., Elliot, S. L., & Hughes, D. P. (2011). Hidden diversity behind the zombie-ant fungus *Ophiocordyceps unilateralis*: four new species described from carpenter ants in Minas Gerais, Brazil. *PloS one*, *6*(3), e17024. doi:10.1371/journal.pone.0017024
- Fisher, M. C., Henk, D. A., Briggs, C. J., Brownstein, J. S., Madoff, L. C., McCraw, S. L., & Gurr, S. J. (2012). Emerging fungal threats to animal, plant and ecosystem health. *Nature*, *484*(7393), 186-194. doi:10.1038/nature10947
- Frick, W. F., Pollock, J. F., Hicks, A. C., Langwig, K. E., Reynolds, D. S., Turner, G. G., . . . Kunz, T. H. (2010). An Emerging Disease Causes Regional Population Collapse of a Common North American Bat Species. *Science*, *329*(5992), 679-682. doi:10.1126/science.1188594
- Garcia-Vidal, C., Viasus, D., & Carratalà, J. (2013). Pathogenesis of invasive fungal infections. *Current opinion in infectious diseases*, *26*(3), 270.
- Goriely, A., & Tabor, M. (2006). Estimates of biomechanical forces in *Magnaporthe oryzae*. *Mycological Research*, *110*(7), 755-759. doi:10.1016/j.mycres.2006.03.014
- Grahl, N., Shepardson, K. M., Chung, D., & Cramer, R. A. (2012). Hypoxia and Fungal Pathogenesis: To Air or Not To Air? *Eukaryotic Cell*, *11*(5), 560-570. doi:10.1128/EC.00031-12
- Grist, S. M., Chrostowski, L., & Cheung, K. C. (2010). Optical oxygen sensors for applications in microfluidic cell culture. *Sensors (Basel, Switzerland)*, *10*(10), 9286-9316. doi:10.3390/s101009286
- Grünwald, N. J., Goss, E. M., & Press, C. M. (2008). *Phytophthora ramorum*: a pathogen with a remarkably wide host range causing sudden oak death on oaks and ramorum blight on woody ornamentals. *Molecular Plant Pathology*, *9*(6), 729-740. doi:10.1111/j.1364-3703.2008.00500.x

- Gupta, M., Kocgozlu, L., Sarangi, B. R., Margadant, F., Ashraf, M., & Ladoux, B. (2015). Micropillar substrates: a tool for studying cell mechanobiology. *Methods in cell biology*, 125, 289.
- Hanson, K. L., Nicolau, J. D. V., Filipponi, L., Wang, L., Lee, A. P., & Nicolau, D. V. (2006). Fungi use efficient algorithms for the exploration of microfluidic networks. *Small (Weinheim an der Bergstrasse, Germany)*, 2(10), 1212-1220. doi:10.1002/smll.200600105
- Harold, F. M. (1997). How hyphae grow: Morphogenesis explained? *Protoplasma*, 197(3), 137-147. doi:10.1007/BF01288023
- Heath, I. B., & Geitmann, A. (2000). Cell Biology of Plant and Fungal Tip Growth -- Getting to the Point. *The Plant Cell*, 12(9), 1513-1517. doi:10.1105/tpc.12.9.1513
- Henry, W. (1800). Experiments on the Quantity of Gases Absorbed by Water, at Different Temperatures, and under Different Pressures. *Proceedings of the Royal Society of London (1854-1905)*, 1, 103-104. doi:10.1098/rspl.1800.0063
- Hibbett, D. S. (2012). 21st Century Guidebook to Fungi. *The Quarterly Review of Biology*, 87(4), 396-396. doi:10.1086/668171
- Hughes, A. L., Todd, B. L., & Espenshade, P. J. (2005). SREBP Pathway Responds to Sterols and Functions as an Oxygen Sensor in Fission Yeast. *Cell*, 120(6), 831-842. doi:10.1016/j.cell.2005.01.012
- Ibrahim-Granet, O., Jouvion, G., Hohl, T. M., Droin-Bergère, S., Philippart, F., Kim, O. Y., . . . Brock, M. (2010). In vivo bioluminescence imaging and histopathologic analysis reveal distinct roles for resident and recruited immune effector cells in defense against invasive aspergillosis. *BMC microbiology*, 10(1), 105-105. doi:10.1186/1471-2180-10-105
- Jackson, M. A., Jackson, M. A., Dunlap, C. A., Dunlap, C. A., Jaronski, S. T., & Jaronski, S. T. (2010). Ecological considerations in producing and formulating fungal entomopathogens for use in insect biocontrol. *BioControl*, 55(1), 129-145. doi:10.1007/s10526-009-9240-y
- Jain, M., & Sznajder, J. I. (2005). Effects of hypoxia on the alveolar epithelium. *Proceedings of the American Thoracic Society*, 2(3), 202.
- Jeon, H., Simon, C. G., & Kim, G. (2014). A mini-review: Cell response to microscale, nanoscale, and hierarchical patterning of surface structure: A Mini-Review. *Journal of Biomedical Materials Research Part B: Applied Biomaterials*, 102(7), 1580-1594. doi:10.1002/jbm.b.33158
- Johari, S., Nock, V., Alkaisi, M. M., & Wang, W. (2013). On-chip analysis of C. elegans muscular forces and locomotion patterns in microstructured environments. *Lab on a chip*, 13(9), 1699. doi:10.1039/c3lc41403e

- Karabanova, L. V., Mikhlovskaya, S. V., Sergeeva, L. M., Meikle, S. T., Helias, M., & Lloyd, W. (2004). Semi-interpenetrating polymer networks based on polyurethane and poly(vinyl pyrrolidone) obtained by photopolymerization: Structure-property relationships and bacterial adhesion. *Polymer Engineering & Science*, 44(5), 940-947. doi:10.1002/pen.20085
- Karhausen, J., Furuta, G. T., Tomaszewski, J. E., Johnson, R. S., Colgan, S. P., & Haase, V. H. (2004). Epithelial hypoxia-inducible factor-1 is protective in murine experimental colitis. *The Journal of clinical investigation*, 114(8), 1098-1106. doi:10.1172/JCI200421086
- Kim, K., & Harvell, C. D. (2004). The Rise and Fall of a Six-Year Coral-Fungal Epizootic. *The American Naturalist*, 164(S5), S52-S63. doi:10.1086/424609
- Kohlmeier, T., & Gatzert, H. H. (2002). Challenges in using photosensitive embedding material to planarize multi-layer coils for actuator systems. *Journal of Magnetism and Magnetic Materials*, 242, 1149-1152. doi:10.1016/S0304-8853(01)01303-8
- Lerman, M. J., Lembong, J., Muramoto, S., Gillen, G., & Fisher, J. P. (2018). The Evolution of Polystyrene as a Cell Culture Material. *Tissue Engineering Part B: Reviews*. doi:10.1089/ten.TEB.2018.0056
- Lew, R. R. (2011). How does a hypha grow? The biophysics of pressurized growth in fungi. *Nature Reviews Microbiology*, 9(7), 509-518. doi:10.1038/nrmicro2591
- Lew, R. R., Levina, N. N., Walker, S. K., & Garrill, A. (2004). Turgor regulation in hyphal organisms. *Fungal Genetics and Biology*, 41(11), 1007-1015. doi:10.1016/j.fgb.2004.07.007
- Li, N., Tourovskaia, A., & Folch, A. (2003). Biology on a chip: microfabrication for studying the behavior of cultured cells. *Critical reviews in biomedical engineering*, 31(5-6), 423.
- Lorch, J. M., Meteyer, C. U., Behr, M. J., Boyles, J. G., Cryan, P. M., Hicks, A. C., . . . Blehert, D. S. (2011). Experimental infection of bats with *Geomyces destructans* causes white-nose syndrome. *Nature*, 480(7377), 376-378. doi:10.1038/nature10590
- Maček, I., Dumbrell, A. J., Nelson, M., Fitter, A. H., Vodnik, D., & Helgason, T. (2011). Local Adaptation to Soil Hypoxia Determines the Structure of an Arbuscular Mycorrhizal Fungal Community in Roots from Natural CO₂ Springs. *Applied and Environmental Microbiology*, 77(14), 4770-4777. doi:10.1128/AEM.00139-11
- McCormick, A., Jacobsen, I. D., Broniszewska, M., Beck, J., Heesemann, J., & Ebel, F. (2012). The Two-Component Sensor Kinase TcsC and Its Role in Stress Resistance of the Human-Pathogenic Mold *Aspergillus fumigatus*. *PloS one*, 7(6), e38262. doi:10.1371/journal.pone.0038262

- McKerracher, L. J., & Heath, I. B. (1987). Cytoplasmic migration and intracellular organelle movements during tip growth of fungal hyphae. *Experimental Mycology*, *11*(2), 79-100. doi:10.1016/0147-5975(87)90041-7
- Mehta, G., Mehta, G., Mehta, K., Mehta, K., Sud, D., Sud, D., . . . Takayama, S. (2007). Quantitative measurement and control of oxygen levels in microfluidic poly(dimethylsiloxane) bioreactors during cell culture. *Biomedical Microdevices*, *9*(2), 123-134. doi:10.1007/s10544-006-9005-7
- Monahan, J., Gewirth, A. A., & Nuzzo, R. G. (2001). A Method for Filling Complex Polymeric Microfluidic Devices and Arrays. *Analytical Chemistry*, *73*(13), 3193-3197. doi:10.1021/ac001426z
- Money, N. P. (1990). Measurement of hyphal turgor. *Experimental Mycology*, *14*(4), 416-425. doi:10.1016/0147-5975(90)90064-Z
- Muralidhar, A., Swadel, E., Spiekerman, M., Suei, S., Fraser, M., Ingerfeld, M., . . . Garrill, A. (2016). A pressure gradient facilitates mass flow in the oomycete *Achlya bisexualis*. *Microbiology (Reading, England)*, *162*(2), 206-213. doi:10.1099/mic.0.000216
- Nezhad, A. S., Naghavi, M., Packirisamy, M., Bhat, R., & Geitmann, A. (2013a). Quantification of cellular penetrative forces using lab-on-a-chip technology and finite element modeling. *Proceedings of the National Academy of Sciences of the United States of America*, *110*(20), 8093-8098. doi:10.1073/pnas.1221677110
- Nezhad, A. S., Naghavi, M., Packirisamy, M., Bhat, R., & Geitmann, A. (2013b). Quantification of the Young's modulus of the primary plant cell wall using Bending-Lab-On-Chip (BLOC). *Lab on a chip*, *13*(13), 2599-2268. doi:10.1039/c3lc00012e
- Nizet, V., & Johnson, R. S. (2009). Interdependence of hypoxic and innate immune responses. *Nature Reviews Immunology*, *9*(9), 609-617. doi:10.1038/nri2607
- Nock, V., Alkaisi, M., & Blaikie, R. J. (2010). Photolithographic patterning of polymer-encapsulated optical oxygen sensors. *Microelectronic Engineering*, *87*(5), 814-816. doi:10.1016/j.mee.2009.11.076
- Nock, V., Tayagui, A., & Garrill, A. (2015). Elastomeric micropillar arrays for the study of protrusive forces in hyphal invasion. In: University of Canterbury. Biological Sciences.
- Orcheston-Findlay, L., Hashemi, A., Garrill, A., & Nock, V. (2018). A microfluidic gradient generator to simulate the oxygen microenvironment in cancer cell culture. *Microelectronic Engineering*, *195*, 107-113. doi:10.1016/j.mee.2018.04.011

- Orcheston-Findlay, L., Hashemi, A., Nock, V., & Garrill, A. (2018). PVP treatment of PS/PtOEPK sensor films for improved adherence of cancer cells. *International Journal of Nanotechnology*, *15*(8-10), 753-759. doi:10.1504/IJNT.2018.098444
- Pennisi, E. (2010). Armed and Dangerous. *Science*, *327*(5967), 804-805. doi:10.1126/science.327.5967.804
- Phillips, A. J., Anderson, V. L., Robertson, E. J., Secombes, C. J., & van West, P. (2008). New insights into animal pathogenic oomycetes. *Trends in Microbiology*, *16*(1), 13-19. doi:10.1016/j.tim.2007.10.013
- Raymond, J., & Segrè, D. (2006). The Effect of Oxygen on Biochemical Networks and the Evolution of Complex Life. *Science*, *311*(5768), 1764-1767. doi:10.1126/science.1118439
- Rizzo, D. M., & Garbelotto, M. (2003). Sudden Oak Death: Endangering California and Oregon Forest Ecosystems. *Frontiers in Ecology and the Environment*, *1*(4), 197-204. doi:10.1890/1540-9295(2003)001[0197:SODECA]2.0.CO;2
- Rozpędowska, E., Galafassi, S., Johansson, L., Hagman, A., Piškur, J., Compagno, C., . . . Biologiska, i. (2011). *Candida albicans*— a pre-whole genome duplication yeast – is predominantly aerobic and a poor ethanol producer. *FEMS Yeast Research*, *11*(3), 285-291. doi:10.1111/j.1567-1364.2010.00715.x
- Sanati Nezhad, A., & Geitmann, A. (2013). The cellular mechanics of an invasive lifestyle. *Journal of experimental botany*, *64*(15), 4709-4728. doi:10.1093/jxb/ert254
- Siddique, A., Meckel, T., Stark, R. W., & Narayan, S. (2017). Improved cell adhesion under shear stress in PDMS microfluidic devices. *Colloids and Surfaces B: Biointerfaces*, *150*, 456-464. doi:10.1016/j.colsurfb.2016.11.011
- Singh, A., Freeman, B. D., & Pinnau, I. (1998). Pure and mixed gas acetone/nitrogen permeation properties of polydimethylsiloxane [PDMS]. *Journal of Polymer Science Part B: Polymer Physics*, *36*(2), 289-301. doi:10.1002/(SICI)1099-0488(19980130)36:2<289::AID-POLB8>3.0.CO;2-M
- Stanley, C. E., Grossmann, G., Casadevall i Solvas, X., & deMello, A. J. (2016). Soil-on-a-Chip: microfluidic platforms for environmental organismal studies. *Lab on a chip*, *16*(2), 228-241. doi:10.1039/c5lc01285f
- Sud, D., Zhong, W., Beer, D. G., & Mycek, M.-A. (2006). Time-resolved optical imaging provides a molecular snapshot of altered metabolic function in living human cancer cell models. *Optics express*, *14*(10), 4412. doi:10.1364/OE.14.004412

- Sun, S., Ungerböck, B., & Mayr, T. (2015). Imaging of oxygen in microreactors and microfluidic systems. *Methods and applications in fluorescence*, 3(3), 034002. doi:10.1088/2050-6120/3/3/034002
- Sun, W., Chen, Y., Wang, Y., Luo, P., Zhang, M., Zhang, H., & Hu, P. (2018). Interaction study of cancer cells and fibroblasts on a spatially confined oxygen gradient microfluidic chip to investigate the tumor microenvironment. *The Analyst*, 143(22), 5431-5437. doi:10.1039/C8AN01216D
- Takeshita, N. (2016). Coordinated process of polarized growth in filamentous fungi. *Bioscience, Biotechnology, and Biochemistry*, 80(9), 1693-1699. doi:10.1080/09168451.2016.1179092
- Tayagui, A., Sun, Y., Collings, D. A., Garrill, A., & Nock, V. (2017). An elastomeric micropillar platform for the study of protrusive forces in hyphal invasion. *Lab on a chip*, 17(21), 3643-3653. doi:10.1039/C7LC00725F
- Thomson, D. D., Wehmeier, S., Byfield, F. J., Janmey, P. A., Caballero-Lima, D., Crossley, A., & Brand, A. C. (2015). Contact-induced apical asymmetry drives the thigmotropic responses of *Candida albicans* hyphae. *Cellular Microbiology*, 17(3), 342-354. doi:10.1111/cmi.12369
- Todd, B. L., Stewart, E. V., Burg, J. S., Hughes, A. L., & Espenshade, P. J. (2006). Sterol Regulatory Element Binding Protein Is a Principal Regulator of Anaerobic Gene Expression in Fission Yeast. *Molecular and Cellular Biology*, 26(7), 2817-2831. doi:10.1128/MCB.26.7.2817-2831.2006
- Tremblay, P., Savard, M. M., Vermette, J., & Paquin, R. (2006). Gas permeability, diffusivity and solubility of nitrogen, helium, methane, carbon dioxide and formaldehyde in dense polymeric membranes using a new on-line permeation apparatus. *Journal of Membrane Science*, 282(1), 245-256. doi:10.1016/j.memsci.2006.05.030
- Tyler, W. J. (2012). The mechanobiology of brain function. *Nature reviews. Neuroscience*, 13(12), 867-878. doi:10.1038/nrn3383
- Uchida, M., Bartnicki-García, S., & Roberson, R. W. (2004). Mechanisms of Hyphal Tip Growth and Morphogenesis in the Filamentous Fungus *Neurospora crassa*. *Microscopy and Microanalysis*, 10(S02), 1554-1555. doi:10.1017/S1431927604886604
- Valderrama, J. O., Campusano, R. A., & Forero, L. A. (2016). A new generalized Henry-Setschenow equation for predicting the solubility of air gases (oxygen, nitrogen and argon) in seawater and saline solutions. *Journal of Molecular Liquids*, 222, 1218-1227. doi:10.1016/j.molliq.2016.07.110
- Voldman, J., Gray, M. L., & Schmidt, M. A. (1999). Microfabrication in Biology and Medicine. *Annual Review of Biomedical Engineering*, 1(1), 401-425. doi:10.1146/annurev.bioeng.1.1.401

- Walker, S. K., Chitcholtan, K., Yu, Y., Christenhusz, G. M., & Garrill, A. (2006). Invasive hyphal growth: An F-actin depleted zone is associated with invasive hyphae of the oomycetes *Achlya bisexualis* and *Phytophthora cinnamomi*. *Fungal Genetics and Biology*, 43(5), 357-365. doi:10.1016/j.fgb.2006.01.004
- Wang, W., Wang, X., Liu, J., Ishii, M., Igarashi, Y., & Cui, Z. (2007). Effect of Oxygen Concentration on the Composting Process and Maturity. *Compost Science & Utilization*, 15(3), 184-190. doi:10.1080/1065657X.2007.10702331
- Willger, S. D., Puttikamonkul, S., Kim, K.-H., Burritt, J. B., Grahl, N., Metzler, L. J., . . . Cramer, J. R. A. (2008). A sterol-regulatory element binding protein is required for cell polarity, hypoxia adaptation, azole drug resistance, and virulence in *Aspergillus fumigatus*. *PLoS pathogens*, 4(11), e1000200. doi:10.1371/journal.ppat.1000200
- Wills, R. T. (1993). THE ECOLOGICAL IMPACT OF PHYTOPHTHORA-CINNAMOMI IN THE STIRLING-RANGE-NATIONAL-PARK, WESTERN-AUSTRALIA. *Australian Journal of Ecology*, 18(2), 145-159. doi:10.1111/j.1442-9993.1993.tb00439.x
- Wu, C.-C., Yasukawa, T., Shiku, H., & Matsue, T. (2005). Fabrication of miniature Clark oxygen sensor integrated with microstructure. *Sensors & Actuators: B. Chemical*, 110(2), 342-349. doi:10.1016/j.snb.2005.02.014
- Xia, Y., & Whitesides, G. M. (1998). Soft lithography. *Annual Review of Materials Science*, 28, 153.
- Yang, W., Luo, C., Lai, L., & Ouyang, Q. (2015). A novel microfluidic platform for studying mammalian cell chemotaxis in different oxygen environments under zero-flow conditions. *Biomicrofluidics*, 9(4), 044121. doi:10.1063/1.4929406